Characterization of Somatic Mutations in mTOR Pathway Genes in Focal Cortical Dysplasias

Eric Krochmalnek
Integrated Program in Neuroscience
McGill University, Montreal
June 2021

Thesis submitted to McGill University
in partial fulfillment of the requirements of the degree
of Master of Science

Table of Contents

I. Abstract

Focal cortical dysplasias (FCDs) are focal structural abnormalities of the brain caused by defects in neuronal migration, proliferation and differentiation during development.[1] FCDs represent the most common cause of focal drug-resistant epilepsy, accounting for ≈15- 25% of all cases, which can often lead to catastrophic morbidity with a heavy burden for patients and families.[2,3] Seizures usually appear in early infancy or childhood, but some experience their first seizure during adulthood.[2,4] Currently available antiepileptic medications are ineffective and nonspecific, with ≈50% of FCD patients having persistent uncontrolled seizures.[5] Unfortunately, surgical resection is only possible in a subset of patients and the pathophysiology of FCD remains poorly understood.[3] Remarkably, several studies have found that somatic mutations, which arise in the embryo after fertilization, in genes of the mechanistic target of rapamycin (mTOR) pathway, are responsible for some types of FCDs.[2,3,6] These mutations are present in a very small proportion of cells, ranging from ≈2-10% within FCD tissue, and result in mTOR pathway hyperactivation.[2,3] Screening for low-level somatic variants in FCD is not done on a clinical basis and requires ultra-deep genetic sequencing of DNA directly extracted from affected brain tissue.[6] Presently, the underlying cause of FCD is found in 15.6-57% of surgical tissue specimens.[6,7] However, the diagnostic yield and topographic distribution of somatic mTOR pathway mutations in FCD remain unclear.[6] In this study, we perform targeted ultra-deep sequencing using a custom mTOR pathway gene panel on resected histopathologically confirmed FCD brain tissue specimens from 24 patients to determine the prevalence and spatial distribution of FCDs that are due to low-level somatic mTOR pathway mutations. We successfully identified causal variants in 58% (14/24) of patients and revealed that the allelic frequency of somatic mutations correlates with FCD lesion size and histopathological severity.

Moreover, we described and confirmed, by functional in vitro studies, two novel previously unreported variants involved in mTOR pathway hyperactivation and FCD pathogenesis. This study illustrates the convergence between histopathology, brain topography and somatic mTOR pathway mutations, with the goal of enhancing patient care and management, especially given that there are clinically available drugs targeting the mTOR pathway.[8]

II. Résumé

Les dysplasies corticales focales sont des anomalies structurelles focales du cerveau causées par des anomalies de migration, de prolifération et de différenciation des neurones durant le développement.[1] La dysplasie corticale focale est la cause la plus fréquente d'épilepsie focale résistante aux médicaments, représentant ≈15 à 25% des cas.[3] Elle est souvent associée à une morbidité catastrophique constituant un lourd fardeau pour les patients et leurs familles.[2] Les crises d'épilepsie apparaissent généralement durant l'enfance, mais quelques patients peuvent voir apparaitre leur première crise à l'âge adulte. [2,4] Les antiépileptiques présentement disponibles sont inefficaces et non spécifiques pour environ 50% des patients.[5] La résection chirurgicale de la lésion n'est toutefois possible que pour un sous-ensemble de patients, et les mécanismes physiopathologiques de la dysplasie corticale focale demeurent encore mal compris.[3] Plusieurs études ont montré que des mutations somatiques post-zygotiques des gènes de la voie mTOR, sont responsables de quelques dysplasies corticales focales.[2,3,6] Ces mutations sont présentes dans environ 2 à 10% des cellules du tissu dysplasique provoquant une hyperactivation de la voie mTOR. [2,3] Les tests génétiques ciblés pour la détection de ces mutations somatiques ne sont pas systématiquement disponibles en clinique et nécessitent un séquençage génétique très sensible de l'ADN directement extrait du tissu cérébral affecté.[6] En effet, plusieurs travaux rapportent la présence de ces mutations dans 15,6 à 57% des tissus chirurgicaux.[6,7] Par ailleurs, le rendement diagnostique et la distribution topographique de ces variants somatiques de la voie mTOR dans la dysplasie corticale focale ne sont pas très bien répertoriés.[6] Le but de ce présent travail est de réaliser, sur des échantillons cérébraux de 24 patients ayant un diagnostic histopathologique de dysplasie corticale focale, un séquençage ciblé d'une grande profondeur à l'aide d'un panel de gènes de la voie mTOR. Ceci permettra de déterminer la prévalence et la distribution spatiale des

mutations somatiques de la voie mTOR à l'origine de ces dysplasies corticales focales. Nous avons identifié les mutations causales chez 58% (14/24) des patients et avons montré une corrélation entre la fréquence allélique des mutations somatiques et la sévérité histopathologique de la dysplasie corticale. De plus, nous avons décrit et confirmé, par des études fonctionnelles in vitro, deux nouveaux variants impliqués dans l'hyperactivation de la voie mTOR et par conséquent, dans la pathogenèse de la dysplasie corticale focale. Ces résultats soulignent la convergence des données histopathologiques avec la fréquence et la répartition topographique des mutations somatiques de la voie mTOR pour améliorer les soins et la prise en charge des patients parce qu'il existe des médicaments disponibles en clinique qui contrôlent l'hyperactivation de la voie mTOR.[8]

III. Acknowledgements

First and foremost, I would like to thank Dr. Myriam Srour who warmly introduced me to her lab and gave me the extraordinary opportunity to embark on this project. Dr. Srour's positivity, dedication and invaluable feedback were indispensable in making this study a resounding success by providing the wholehearted support that many would only hope to find in a supervisor. I will be forever grateful for the opportunity to share in her knowledge and passion for patient care and clinical research.

I would like to say a special thank you to Judith St-Onge, Nassima Addour and Lina Mougharbel, our research assistants, for all the technical, professional and personal guidance I received during my studies. I also thank Judith St-Onge and Nassima Addour for maintaining the tissue biobank and the opportunity to enhance my French. I am grateful to the neurogenetics fellows Drs. Sarah Alsubhi and Ghadd Alhajaj, who helped cultivate a positive stimulating lab environment.

Thank you to Drs. Roy Dudley, Jeffery Hall, Jean-Pierre Farmer, Alexander Weil, Jeffrey Atkinson and the entire neurosurgery team, without whom, none of this would have been possible. In addition, I thank our many wonderful clinicians and collaborators for coordinating patient recruitment and the opportunity to learn state-of-the-art clinical diagnostic tools. I am extremely grateful to Dr. Nahum Sonenberg for allowing me to study in his lab and meet his wonderfully talented team. I also thank Dr. Andrea Accogli for preliminary testing and mapping of the mTOR panel and for being consistently supportive and eager to exchange new ideas.

I thank Drs. David Rosenblatt and Jean-Baptiste Rivière for their expertise and guidance as part of my advisory committee. In addition, I thank Dusica Maysinger, my IPN mentor, for her outstanding guidance and support.

Thank you to my parents and sister for their unconditional support, who inspired me to go after my dreams.

I also thank the patients and families for their invaluable participation, who helped make this study possible. Moreover, I thank the MUHC bioinformatics platform for its assistance with sequence processing and variant annotation. I also extend my thanks to all the members of the Child Health and Human Development program and the entirety of the MUHC for their hospitality, professionalism, and friendly atmosphere.

Lastly, I am grateful for the many amazing friendships I made along the way, particularly Gyan Prakash, for squash competition inspiration and Meagan Collins for her many funny anecdotes.

My fellowship training was generously supported by the FRQS, McGill University's Faculty of Medicine Fellowship, the Department of Neurology and Neurosurgery Excellence Award, and the MUHC Desjardins Award.

IV. Contributions of Authors

This thesis was written by Eric Krochmalnek and edited by Dr. Myriam Srour and Nassima Addour. Dr. Andrea Accogli and Judith St-Onge conducted preliminary testing of the mTOR gene panel, provided technical support and assisted with MRI mapping. Gyan Prakash and Sunghoon Kim assisted with western blotting and analysis in the Sonenberg lab. All other data processing and analyses were performed by Eric Krochmalnek.

V. List of Abbreviations

4EBP1	eIF4E Binding Protein-1
AAF	Alternate allele frequency
AKT	RAC-alpha serine/threonine-protein kinase
ALS	Amyotrophic lateral sclerosis
ANOVA	Analysis of variance
ASD	Autism spectrum disorder
BC	Balloon cell
BSA	Bovine serum albumin
CCND2	Cyclin D2
CDN	Cytomegalic dysmorphic neuron
ClinVar	Clinical variant database
CLOVES	Congenital lipomatous overgrowth, vascular malformations, epidermal nevi and scoliosis/skeletal/spinal anomalies
COSMIC	Catalogue Of Somatic Mutations In Cancer
CRISPR	Clustered regularly interspaced short palindromic repeats
CUSA	Cavitron ultrasonic surgical aspirator
DEPDC5	DEP domain-containing 5
DMEM	Dulbecco's Modified Eagle Medium
eIF-4E	Eukaryotic translation initiation factor 4E
FBS	Fetal bovine serum
FCD	Focal cortical dysplasia
FFPE	Formalin-Fixed Paraffin-Embedded
FMCD	Focal malformations of cortical development
$GABA_B$	Gamma-aminobutyric acid B
gnomAD	Genome Aggregation Database
HA	Human influenza hemagglutinin
HEK293T	Human embryonic kidney 293 cells of the SV40 large T antigen
HME	Hemimegalencephaly
ID	Intellectual disability

ILAE	International League Against Epilepsy
IL-1R	Interleukin-1 receptor
IRS-1	Insulin receptor substrate 1
MDR1	Multi-Drug Resistance 1
MDRP	Multidrug-resistant proteins
miRNA	MicroRNA
mLST8	Mammalian lethal with Sec13 protein 8
MRP1	Multidrug resistance-associated protein 1
MTORC	mTOR complex 1
NPRL	Nitrogen permease regulator like protein
OVG	Overgrowth
p70-S6K1	P70 ribosomal protein S6 kinase beta-1
pcDNA3	Plasmid cloning DNA3
PDCD4	Programmed cell death protein 4
PDK1	Phosphoinositide-dependent kinase-1
PIK3CA	Phosphatidylinositol-4,5-Bisphosphate 3-Kinase Catalytic Subunit Alpha
PIK3R2	Phosphoinositide-3-Kinase Regulatory Subunit 2
PMG	Polymicrogyria
p-p70-S6K1	Phospho-p70 ribosomal protein S6 kinase beta-1
PTEN	Phosphatase and tensin homolog
Raptor	Regulatory protein associated with mTOR
RGCs	Radial glial cells
RHEB	Ras homolog enriched in brain
Rictor	Rapamycin insensitive companion of mTOR
RPS6	Ribosomal Protein S6
SDS-PAGE	Sodium dodecyl sulphate–polyacrylamide gel electrophoresis
SEM	Standard error of the mean
SLC35A2	Solute Carrier Family 35 Member A2
SNP	Single-nucleotide polymorphism
STRADα	STE20-related kinase adapter protein alpha
TBC1D7	TBC1 Domain Family Member 7

T	Threonine
TLR	Toll-like receptor
TSC	Tuberous sclerosis complex
VZ	Ventricular zone

VI. List of Figures

Chapter 2:

Chapter 4:

Chapter 5:

Chapter 6:

VII. List of Tables

Page

Chapter 5:

Appendices:

Chapter 1: Introduction and Statement of Problem

Approximately 65 million people worldwide have epilepsy, making it one of the most common neurological diseases.[9] Epilepsy comprises a diverse group of neurological disorders of varying severities characterized by recurrent seizures. Epilepsy can develop at any age; however, new cases are commonly observed in children, particularly during their first year of life.[10] Up to 50% of patients diagnosed with epilepsy are idiopathic cases.[11] Seizures can have cognitive, psychosocial, and developmental effects, with an increased risk of physical injury, and sudden unexpected death.[10] Seizures can arise from several factors including faulty neuronal wiring, genetics, inflammation, autoimmune disorders, physical trauma, environmental factors and infection.[12] Although there is no cure for epilepsy, a variety of therapies, including medication, dietary changes, and surgery may be offered to alleviate seizures. Several antiepileptic medications may be needed to regulate electrical activity within the brain, and over 30% of patients with epilepsy do not respond to medication.[13]

Focal malformations of cortical development (FMCD) are congenital structural brain abnormalities that encompass several neurodevelopmental disorders, which include FCD, tuberous sclerosis complex (TSC), and hemimegalencephaly (HME).[14] FCDs are structural abnormalities of brain development caused by defects in neuronal migration, proliferation, and differentiation leading to significant disorganization of the hexalaminar cortical structure, and abnormal neuronal and glial cell morphology.[1]

FCDs are the most prevalent cause of focal drug-resistant epilepsy, representing ≈15-25% of all cases.[3] Unfortunately, ≈50% of FCD patients are refractory to medication and experience persistent uncontrolled seizures.[5] If the FCD is in an accessible, well-defined location, surgical resection of the FCD is offered as treatment. However, many patients are not

surgical candidates and current treatment options are limited, inefficient and often impractical, commonly involving multiple surgical resections.[15]

FCD pathophysiology remains poorly understood and diagnosis and treatment of FCD remain a great challenge.[3] Currently, FCD classification is primarily determined based on a microscopic analysis of surgical brain tissue for histopathological characteristics.[16] However, several studies examining bulk DNA from resected FCD tissue have recently identified somatic mutations, which are mutations arising in the embryo after fertilization, in mTOR signalling pathway genes.[2,3,6,] The mTOR pathway modulates many fundamental cell processes including cell proliferation, growth and migration.[17] Aberrant mTOR pathway signalling is proposed as a critical mechanism accounting for the histopathological features of some types of FCDs.[2,6,18] Somatic mutations within the mTOR pathway only affect approximately 2-10% of the cells in FCDs, thus, they are undetectable by conventional genetic testing methods.[2,3] Therefore, ultra-deep genetic sequencing of the affected brain tissue is crucial to detect low-level somatic mutations in mTOR pathway genes in order to identify patients who may benefit from targeted medical and surgical treatments.[6] Presently, the underlying cause of FCD has only been found in 15.6-57% of samples examined. [6,7] The association of the mTOR pathway in the pathogenesis of FCDs is extremely exciting, as specific therapies targeting the mTOR pathway are available, allowing personalized pathophysiologic-based treatment.[8] However, the diagnostic yield of FCD patients carrying somatic mTOR pathway variants remains unclear.[3,6]

In this study, we use next-generation ultra-deep genetic sequencing of histopathologically confirmed resected FCD tissue in 24 individuals to determine the diagnostic yield and spatial distribution of FCDs that are due to low-level somatic mTOR pathway mutations. This study aims to elucidate the intersection between histopathology, brain topography and somatic mTOR

pathway mutations, to enhance patient care and medical management, especially given that there are clinically available drugs targeting the mTOR pathway.[8]

Chapter 2: Background

2.1 Focal cortical dysplasia:

FCDs are focal malformations of cortical development arising from defects in neuronal migration, proliferation, and differentiation leading to significant disruption of the hexalaminar cortical structure, and abnormal neuronal and/or glial cell morphology.[1] FCD malformation size can range from a few millimetres to several centimetres, often with an indeterminate border between the lesion and the surrounding tissue.[2] Secondary clinical symptoms may result from focal disruption of the brain in the region affected by the FCD, such as language delays with dominant temporal lobe involvement, muscle weakness with frontal lobe and motor cortex involvement or visual impairments with occipital lobe involvement.[4] If the FCD does not overlap with eloquent cortex, and is in an accessible location with well-defined borders, surgical resection of the FCD is offered as treatment.[19] However, 25-50% of patients will continue to have seizures two years post-resection.[15] Furthermore, neurosurgery is associated with significant risk factors, and many patients are not surgical candidates.[20]

2.2 FCD classification:

In 1971, FCD was first described by Taylor et al., in a group of 10 patients with malformations that shared similarities to tubers in TSC.[21] Since then, the FCD classification structure continues to undergo updates as technology and diagnostic techniques evolve.[22]

In 2011, the International League Against Epilepsy (ILAE) classified FCD into 3 main subcategories, FCD type I, II and III, based on microscopic histological presentation. FCD type I is characterized by alterations in radial (FCD type Ia), tangential (FCD type Ib) or both radial and tangential cortical (FCD type Ic) lamination.[23] FCD type II is the most common

malformation subtype[24] and presents with cortical laminar disruption and the appearance of morphologically abnormal cell types, including cytomegalic dysmorphic neurons (CDNs) (FCD type IIa) and balloon cells (BCs) (FCD type IIb). FCD Type III is similar to FCD type I, with an additional brain lesion present such as hippocampal sclerosis (FCD type IIIa), tumours (FCD type IIIb), vascular malformations (FCD type IIIc) or other acquired lesion e.g. trauma (FCD type IIId).[23] Multiple FCD subtypes may occur in the same lesion, and in such cases, the highest numeric classification prevails.[25] However, diagnostic challenges remain while using the 2011 International League Against Epilepsy classification scheme due to the lack of an integrated molecular classification system.[26]

CDNs and BCs are histopathological hallmarks of cortical malformations used to distinguish between FCD subtypes. BCs are not normally present in the cerebral cortex and the developmental origin of BCs remains unknown.[23] BCs express distinct markers of both neuronal and glial lineages. Moreover, BCs and CDNs were found to be nonclonally derived[2], and likely arise from distinct pools of progenitor cells. In FCD type II, BCs provide an insulating effect and do not initiate epileptic activity, whereas CDNs and immature neurons play an important role in the generation and propagation of epileptic discharges.[25]

Mild malformations of cortical development (mMCD), previously known as microdysgenesis, are microscopic malformations of cortical development. mMCD can be categorized by excess heterotopic cortical neurons in layer 1 (mMCD type I) or microscopic neuronal clusters or excess heterotopic single neurons in deep white matter (mMCD type II). It is currently estimated that ≈ 30% of mMCD/FCD1 cases are related to glycosylation defects due to *SLC35A2* pathogenic variants.[6] In addition, newly described histological entities, such as mild

malformation of cortical development with oligodendroglial hyperplasia (MOGHE)[27] and bottom-of-sulcus dysplasia are mMCD that can be characterized with MRI.[16]

2.3 Genetic variants:

Genetic variants are nucleotide changes caused by DNA replication machinery errors or environmental factors. DNA alterations include nucleotide substitutions, deletions and insertions which can alter splice sites and create frameshifts. Environmental factors that can contribute to genetic variants include stress, tobacco, radiation, viruses, chemical exposure, and ageing.[28] Pathogenic variants can affect protein structure and lead to various pathologies by perturbing vital aspects of cellular function.[29] Alternatively, a synonymous nucleotide change does not alter the encoded amino acid and results in a benign variant or silent mutation. Benign variants do not disrupt protein structure or function.[28]

2.4 Somatic and germline variants:

Variants can be broadly classified as either somatic or germline based on their tissue of origin. Somatic variants arise from spontaneous de novo genetic alterations acquired after fertilization and can occur in any cell undergoing division at any stage of life, from the first cleavage of a zygote to the organism's last cell division.[30] Somatic variants are only present in a subset of cells in the organism and are not passed down to future generations unless they occur in the gametes.[31] Conversely, germline variants occur in the parent's gametes and are present in all cells of the offspring.[30] Pathogenic germline variants can be passed down to future generations. Therefore, germline mutations occur pre-zygotically, and are present in all cells of the offspring, while somatic mutations occur post-zygotically, and are present in only the descendants of

mutated cells. Both somatic and germline variants can be classified as either pathogenic or benign.[31]

2.5 Somatic variants in the nervous system:

Somatic variants can occur in the nervous system during division of neural progenitors to produce mutant daughter cells, leading to the formation of a mosaic patchwork of genetically heterogeneous terminally differentiated neurons (Figure 1).[30] DNA errors occurring during S-phase, the synthesis phase of DNA replication, are a commonly observed type of neuronal genetic variation.[32] During cortical development, each round of cell division has the potential to produce somatic variants, creating the potential for a high degree of genetic variability between individual neurons, with the vast majority of somatic variants being benign.[30] The earlier a somatic variant occurs, the greater the proportion of descendant cells that will carry this variant.[33] Additionally, somatic variants occurring in terminally differentiated neurons, which are post-mitotic cells, accumulate over time and can contribute to various neurodegenerative disorders.[32]

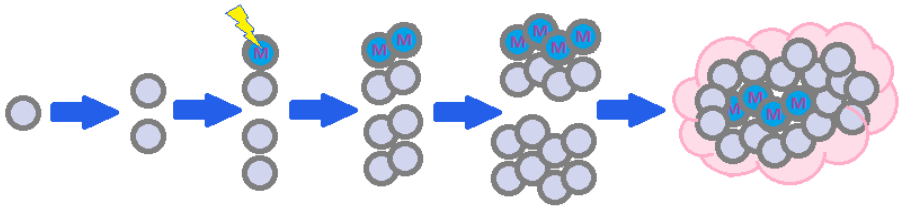

Figure 1: A somatic mutation acquired during embryonic development.
Schematic diagram illustrating somatic mutations occurring during development affect cell descendants, resulting in a focal lesion. The earlier a mutation occurs during embryonic development, the larger the area the mutated cells can cover. M= mutated cell. Lightning bolt= somatic mutation onset.

2.6 Alternate allele frequency:

The alternate allele frequency (AAF) is a percentage measure of the proportion of variant strands to total strands detected during sequencing at a specified nucleotide position. Therefore, the AAF indicates the variant load detected within a given region. The AAF is calculated by dividing the total number of variant strands detected by the total number of strands detected and then multiplying this value by 100.[34]

The AAF provides valuable insight into the number of cells carrying variants within the dysplastic tissue. A cell with a heterozygous variant will produce approximately 50% variant and 50% WT strands, thus, the percentage of affected cells will be approximately double the AAF for a heterozygous variant.[28] For example, a heterozygous somatic variant in FCD tissue with an AAF of 5% indicates that approximately 10% of the patient's cells are carrying the somatic variant. Obtaining an estimate of the number of cells carrying variants can provide valuable insight into the approximate density of variant cells within a given region and their role in FCD pathogenesis.[6]

In FCD type II, approximately 79% of patients have an AAF below 5%.[35] It has recently been suggested that a correlation exists between the somatic variant load and cortical malformation size.[36] Somatic mutations are present at a higher AAF in HME than FCD type II lesions highlighting the significance of mutation timing in the pathogenesis of FMCDs.[6] However, it remains unknown whether a critical fraction of mutated cells is required to contribute to characteristic histopathological FCD hallmarks and epileptogenicity.[35]

2.7 The mTOR signalling pathway:

The mechanistic target of rapamycin (mTOR) is a 289 kDa, highly evolutionarily conserved serine/threonine kinase that is ubiquitously expressed in all eukaryotic cells and is a central player in the mTOR pathway (Figure 2).[7] The mTOR pathway regulates multiple functions including cell growth, proliferation, migration, energy metabolism, autophagy and inflammation. mTOR carries out its multiple functions in coordination with surrounding environmental conditions by sensing levels of nutrients and growth factors. Throughout life, mTOR plays an essential role in allowing cells to grow and divide by regulating the production of proteins, lipids, and nucleotides while also suppressing catabolic pathways such as autophagy.[17] During brain development, the mTOR pathway is involved in the differentiation of neurons and glia and the maintenance of neural stem cell stemness.[37]

mTOR is the catalytic subunit of two distinct protein complexes, mTOR complex 1 (mTORC1) and mTOR complex 2 (mTORC2). mTORC1 is composed of three main components: mTOR, regulatory protein associated with mTOR (Raptor), and mammalian lethal with Sec13 protein 8 (mLST8).[38] mTORC1 is rapamycin sensitive, integrates nutrient inputs and promotes protein synthesis through several downstream signalling cascades, which include ribosomal protein P70-S6 kinase beta-1 (p70-S6K1), eukaryotic translation initiation factor 4E (eIF-4E) and eIF-4E binding protein-1 (4EBP1).[39] mTORC1 facilitates protein synthesis by phosphorylating two key downstream effectors, p70-S6K1 and 4EBP1. p70-S6K1 phosphorylation by mTORC1 occurs directly on its hydrophobic motif, at amino acid position threonine 389, enabling subsequent activation by Phosphoinositide-dependent kinase-1 (PDK1).[40] p70-S6K1 subsequently interacts with several downstream substrates involved with mRNA translation initiation including eIF4B and programmed cell death protein 4 (PDCD4),[41]

which regulates 5′cap binding and enhances the translation efficiency of spliced mRNAs respectively.[38] p70-S6K1 also phosphorylates ribosomal protein S6 (RPS6) a key component of the 40S ribosomal subunit.[42] mTORC2 is insensitive to rapamycin and also contains three main components, mTOR, mLST8 and rapamycin-insensitive companion of mTOR (Rictor).[38] mTORC2 is a tyrosine-protein kinase that promotes the activation of insulin receptors and insulin-like growth factor 1 receptors and is also implicated in the control and maintenance of the actin cytoskeleton and plays a role in cell proliferation and survival.[43] The genetic deletion of either Raptor or Rictor in neurons results in reduced neuronal size, and premature death, highlighting the important role of mTORC1 and mTORC2 in brain development.[38]

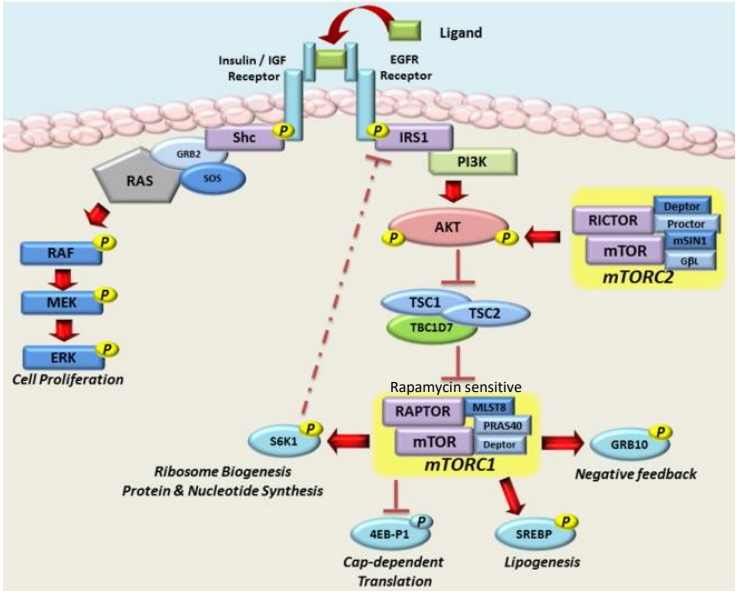

Figure 2: Schematic representation of the mTOR pathway and downstream targets. mTOR forms two distinct protein complexes, mTORC1 and mTORC2. (Adapted. from[17])

2.8 Somatic and germline mutations in the mTOR pathway:

FMCD involving mTOR pathway hyperactivation are classified as mTORopathies, which include FCD, HME and TSC.[44] Both somatic and germline mutations affecting genes of the

mTOR pathway are described as the molecular bases of mTORopathies. Histologically, cortical tuberous lesions in TSC and FCDs are indistinguishable, which helped establish the link between FCD and mTOR pathway dysregulation.[45] Cortical lesions in FCD, TSC and HME share overlapping characteristics and can all contain CDNs and BCs.[46] A single hit, gain of function mutation in mTOR pathway regulatory genes can lead to the upregulation of the mTOR pathway.[39] A two-hit model also exists where a germline loss of function mutation in an mTOR pathway negative regulator is accompanied by a somatic second hit, resulting in biallelic mutations. Biallelic mutations in the same negative regulator gene cause a loss of functional protein, resulting in mTOR pathway upregulation.[33] Hyperphosphorylation of downstream molecules p70-S6K1 and 4EBP1 are characteristic indicators of mTOR pathway upregulation.[2,6]

Hyperactivation of the mTOR pathway is a critical mechanism accounting for the histopathological features of some types of FCDs such as FCD type II.[6] In utero electroporation of activating *MTOR* mutant constructs in mice cause CDNs, disrupted neuronal migration and resulted in spontaneous seizures.[47] Moreover, FCD type II tissue consistently displays strong pS6-immunostaining demonstrating the link between FCD type II and mTORopathies.[6] Recently, synergistic mutations in genes downstream of the mTOR pathway, such as concurrent mutations in *MTOR* and ribosomal protein *RPS6*, have been demonstrated to result in more severe FCD phenotypes.[48] Additionally, the newly described FCD potentially deleterious somatic mutations in the insulin receptor substrate 1 (*IRS-1*) and Ras homolog enriched in brain (*RHEB*) genes have been recently shown to result in mTOR pathway hyperactivation.[42,49] In addition, a study examining somatic *MTOR* mutations in two patients with bottom-of-sulcus dysplasia, a mild form of FCD on MRI, showed that a mutation gradient exists throughout the sulcus, with higher mutation loads at the sulcus bottom compared to the gyral crown. Increased dysmorphic neurons

and balloon cells were also observed in the bottom of the sulcus relative to the gyral crown or adjacent gyri.[16]

Mutations in specific genes within the mTOR pathway have been frequently associated with specific pathological characteristics. For example, *PIK3CA* mutations are commonly found in HME patients, who have larger lesions spanning multiple brain regions.[6] The pathogenicity of *PIK3CA* may depend on the developmental timing of the somatic mutation, where mutations arising in early development have more time to divide and result in a pathogenic phenotype, while somatic mutations arising later in development have less time to divide and may not reach a threshold to result in a pathogenic phenotype.[50] Additionally, mutations in *PIK3CA*, *AKT3* and *RHEB* are frequently associated with poor cognitive outcome, compared to somatic mutations in *MTOR* and *TSC1/2*, or germline mutations in *TSC2* or *DEPDC5* which present with greater variability.[6] Lesion size may also be a contributing factor impacting cognitive outcomes, where larger lesions, as observed in HME, may be coupled with greater cognitive deficits.[50]

Although mTORopathies are often thought to involve hyperactive mTORC1 mediated protein synthesis, mTORC2 may play an important role in the pathophysiology of mTORopathies.[7] Phosphatase and tensin homolog (*PTEN*), a negative regulator of the mTOR pathway, associated with seizures, ASD-like behaviours, macrocephaly and intellectual disability, has also been shown to upregulate mTORC2 activity in the brain of several *PTEN*-deficient individuals.[18] In adolescent *PTEN*-deficient mice, selective antisense oligonucleotide targeting of mTORC2 reversed behavioural and neurophysiological abnormalities by suppressing seizures, rescuing ASD-like behaviours and long-term memory, and normalizing brain metabolic changes.[51] Therefore, mTORC2 may also be a key player contributing to mTOR pathway-related pathophysiology of FCD and therapeutic modulation using a potent and selective mTORC1/2

inhibitor may offer more promising translational applications for treating neurological disorders involving mTORopathies.[8]

2.9 FCD formation during neurodevelopment:

The cerebral cortex is composed of several types of neurons and glia distributed within six layers and organized regionally into highly specialized areas. At the start of corticogenesis, neuroepithelial cells differentiate into radial glial cells (RGCs) that undergo clonal expansion.[52] RGC's can give rise to neurons through either direct neurogenesis or indirect neurogenesis based on the presence of external signals and intrinsic factors. Ventricular zone (VZ) RGC's produce the majority of the excitatory neurons in the neocortex. RGCs have a distinct bipolar morphology with a long basal radial glial fibre and an apical ventricular endfoot to facilitate neuronal migration.[53] The process of inside-out radial migration involves neurons migrating radially along the glial fibres to create a lineage-dependent neocortical microcircuit.[54] Therefore, the inside-out process of corticogenesis results in the cortex having late-born neurons occupy superficial layers of the cortex and early-born neurons occupying deep layers.[53]

FCDs may arise through a spontaneous somatic mutation in a neural progenitor cell during the critical period of corticogenesis occurring between weeks 8–20, when the cortical laminar structure is established.[55] Microdissected FCD cells demonstrate that CDNs and BCs carry pathogenic *MTOR* variants.[6] In addition, binary FACS sorting of neuronal and nonneuronal cells from FCD patients using a neuronal antibody against NeuN revealed mTOR pathway activating mutations were present in the neural population and were expressed variably in the glial population.[44] A proposed developmental and genetic update to the FCD classification

system by Barkovich et al., describes FCD type I as a disorder of abnormal neuronal migration and FCD type II as a disorder of abnormal neuronal and glial proliferation or apoptosis.[56]

2.10 FCD and epileptogenesis:

The molecular mechanisms underlying FCD pathogenesis and epileptogenesis are poorly understood.[6] A seizure is a sudden, uncontrolled electrical imbalance in the brain that can affect behaviour, movement, consciousness, and feelings.[4] Seizures result from aberrant synchronized firing of populations of brain neurons primarily due to an imbalance between excitatory and inhibitory neurotransmission.[9]

There are 3 main categories of seizures. Generalized onset seizures, which affect both sides of the brain simultaneously, focal onset seizures, which originate in one area or group of cells on one side of the brain and unknown onset seizures, which have an unknown seizure origin.[57] Experiencing two or more seizures in the absence of an identifiable cause that occur at least 24 hours apart is generally considered epilepsy.[58]

Most conventional antiepileptic drugs act broadly by decreasing excitation or enhancing inhibition of neural networks.[59] If seizures are intractable to medication, one, or often multiple surgeries are needed to alleviate seizures.[3] The de facto standard method to classify postoperative epilepsy surgery outcomes was developed by Jerome Engel, who described four main classes of potential postoperative outcomes, which are: Class I free of disabling seizures, Class II rare disabling seizures, Class III worthwhile improvement and Class IV no worthwhile improvement respectively.[60]

2.11 Pharmacologic regulation of the mTOR pathway:

Fortunately, there are significant efforts to target the mTOR pathway in FMCD mTORopathies.[61] Several mTOR inhibitors are available that differentially modulate the mTOR pathway. Rapamycin and its analogs such as temsirolimus and everolimus are the most widely used pharmacologic agents to inhibit mTOR.[8] Rapamycin was discovered in 1964 in soil samples collected by a Canadian expedition to the isolated South Pacific island of Rapa Nui and inhibits the mTOR pathway by binding directly to mTOR Complex 1.[38] Inhibition of the mTOR pathway with rapamycin prevented morphological changes and suppressed seizures in mice containing in utero electroporated of activating *MTOR* mutant constructs.[47] Torin1 inhibits the kinase function by acting as an ATP-competitive inhibitor of mTOR, directly blocking phosphorylation.[61,62] INK128 or MLN0128, is a second-generation potent and selective active-site mTOR inhibitor, undergoing clinical trials in cancer, that results in dephosphorylation of downstream mTOR targets p70-S6K1 and 4EBP1.[8] INK128 is a selective kinase inhibitor that targets both mTORC1 and 2 with high efficiency.[63]

Recently, mTOR inhibitors are emerging as effective tools in the management of related mTORopathies.[64,65] TSC, an autosomal dominant neurodevelopmental disorder associated with the growth of non-cancerous tumours in the brain and on other vital organs, is due to mTOR pathway germline mutations in either *TSC1* or *TSC2*, followed by a suspected somatic second hit in tuberous lesions.[14] In TSC, pharmacologic modulation with mTOR inhibitors such as everolimus, have been effective in shrinking tuberous lesions and alleviating epilepsy, leading to their approval for use in some patients.[65]

2.12 FCD Pathophysiology:

It remains unknown how few mosaic cells within a genetically heterogeneous FCD result in intractable epilepsy. Hyperactive mTOR pathway signalling can result in cytomegaly which may compromise cell motility.[66] Hyperactivation of the mTOR pathway in mice increased neuronal size and promoted larger capacitance, resulting in an overall decrease in threshold and increase in action potential firing rates.[67] In addition, dysplastic neurons in FCD exhibit increased calcium influx and calcium currents upon depolarization.[68] Furthermore, the altered expression of neurotransmitter receptors in FCD tissues such as the $GABA_B$ receptor, results in altered GABA function[69] and decreased neuronal hyperpolarization.[70] Mutations in the mTOR pathway may also lead to changes in releasable factors, neurotransmitters, and other modulators that alter cell shape and motility in adjacent, unaffected cells.[2] Therefore, both cell-autonomous and non-cell-autonomous effects may influence cytoarchitecture disruption.[7]

Mutations in the mTOR pathway have also been shown to result in disruption of neuronal ciliogenesis in FCD, leading to cortical dyslamination by compromising Wnt signalling which is essential for neuronal polarization during development.[71] In addition, FCD type II is frequently observed in extratemporal regions and is often located towards the frontal lobe.[22]

In utero electroporation studies in mouse cortical neurons of low, intermediate, and high concentrations of constitutively active *RHEB* induced mTOR pathway hyperactivation, produced spontaneous seizures and increased neuronal soma size and misplacement in a dose-dependent manner. Therefore, the level of neuronal mTOR pathway upregulation correlates with the severity of epilepsy and associated neuropathological characteristics in experimental models TSC and FCD.[72]

Furthermore, differential microRNA (miRNA) expression, which has recently been detected in bulk FCD type II tissue, targets genes in the Hippo signalling pathway involved in the control of organ size through the regulation of cell proliferation and apoptosis.[73] miRNAs are 20–22 nucleotide double-stranded noncoding RNA molecules which can control mRNA translation and degradation.[28] miRNAs are often described as master regulators of gene expression since a single miRNA can influence multiple genes and proteins within diverse molecular pathways. Differential expression of four circulating miRNAs, miR194-2-5p, miR15a-5p, miR-132-3p, and miR-145-5p, extracted from serum exosomes were found to be upregulated in FCD patients compared to controls.[74] Failure of neuronal maturation and migration can lead to mal-developed synaptic circuits, where normal-appearing neurons may be affected by adjacent abnormal cells.[69]

In addition, neurons and glia work together in complex, interdependent networks and are emerging as a highly influential component of the neuronal microenvironment, accounting for various factors such as inflammation and excitation, which may play a key role in the etiology of epilepsy.[69] In TSC, glial dysfunction in humans and mice demonstrate the role of astrocytes, microglia, and oligodendrocytes as major players in the pathophysiology of epilepsy through cell-autonomous and neural-glial interactions. Glial abnormalities such as astrogliosis can affect neuronal function through multiple mechanisms, which include impaired potassium and glutamate homeostasis, inflammatory processes, synaptic remodelling and hypomyelination, which may contribute to TSC features such as epilepsy and intellectual disability.[70]

Neuroinflammation may also contribute to neuronal hyperexcitability underlying seizures, cell death, and neurologic comorbidities.[18] A key upstream generator of the neuroinflammatory response, Interleukin-1 receptor/Toll-like receptor (IL-1R/TLR) signalling, is

induced in FCD. Pro-inflammatory mediators may act as neuromodulators that affect neuronal excitability through nonconventional intracellular signalling pathways. For example, cytokines can modify glutamate and GABA receptor trafficking and subunit assembly.[75] Moreover, transgenic mice with an impaired IL-1R1/TLR4 signalling pathway showed a significant reduction in seizure susceptibility and/or spontaneous seizure recurrence.[76] Inflammatory processes may act in concert with the mechanisms of FCD-related epilepsy and overlapping elements may be at play. Interestingly, despite similar seizure frequency, the inflammatory milieu between FCD type I and II is different in the extent and type of inflammatory mediators detected. In addition, drugs targeting inflammatory pathways are presently in use for patients with autoinflammatory or autoimmune diseases and FCD related epilepsy.[75]

An additional mechanism that may explain drug-resistant epilepsy in FCD is the overexpression of multidrug resistance gene-1 p-glycoprotein (MDR1) and multidrug resistance-associated protein-1 (MRP1) in epileptogenic tissue. Multidrug-resistant proteins (MDRP) may cause medication resistance by expelling antiepileptic drugs from the nervous system, reducing the effective concentration in the brain.[68]

2.13 Using next-generation sequencing technologies to study FCD pathogenesis:

In the past, the study of FCD was very challenging due to the mutation affecting few cells within a heterogeneous lesion. However, with revolutionary next-generation technologies, we can now detect low-level somatic mutations within bulk FCD tissue.[6]

Ultra-deep next-generation sequencing of affected brain tissue using a custom mTOR pathway gene panel is a powerful diagnostic tool that can detect somatic variants present at below 1%[77] which is considerably higher than standard genetic sequencing methods such as

Sanger, with a detection threshold of around 15%.[78] Therefore, low-level somatic variants present at previously undetectable levels can now be identified to assess the diagnostic yield of FCD patients with mTOR pathway mutations. Performing ultra-deep genetic sequencing is crucial to detect low-level somatic mutations in mTOR pathway genes to identify patients who may benefit from targeted medical and potential future surgical intervention.[6,77] Furthermore, understanding the mutation spatial distribution may optimize surgical resection and improve postoperative outcomes.

Chapter 3: Study Objectives

3.1 Rationale for the Study:

FCDs are the most common causes of catastrophic, drug-resistant focal epilepsy in children and adults. Recent studies have revealed that somatic mTOR pathway mutations, which only affect ≈2-10% of the cells, underlie many FCDs.[2,3] However, FCD pathogenesis remains poorly understood, and several key questions remain unanswered. It is unclear what percentage of FCD patients carry somatic mTOR pathway mutations and their topographic distribution throughout the resected brain. Moreover, the role of novel mTOR pathway candidate variants in FCD has yet to be characterized. Additionally, the correlation between the AAF and histopathological changes remains elusive.[3] We are currently at a time when these questions can finally be answered, using novel next-generation technologies and *in vitro* transfection assays. Answering these questions has become essential, given the availability of pathophysiology-specific targeted treatments, such as rapamycin.[8,65]

3.2 Study Aims:

The overarching goal of this study is to understand the pathophysiology of FCD. Our specific aims are:

Aim 1: To investigate the contribution of low-level somatic mutations in FCD pathogenesis by performing ultra-deep genetic sequencing on resected fresh-frozen histopathologically confirmed FCD tissue in 24 individuals and correlate the topographic distribution of mutation load with histology, MRI images and post-surgical outcomes.

Aim 2: To functionally validate unreported candidate variants identified in aim 1 for their role in mTOR pathway hyperactivation using site-directed mutagenesis and *in vitro* transient co-transfection to screen for known mTOR pathway upregulation markers such as hyperphosphorylated p70-S6K1.

3.3 Study Hypotheses:

Hypothesis 1: Ultra-deep sequencing with an updated panel will a) uncover a higher proportion of FCDs due to somatic mutations in mTOR pathway genes than previously published, and b) mutation loads will correlate with MRI lesion size, degree of histopathological severity and reveal a tolerable mutation threshold.

Hypothesis 2: In vitro functional assays of previously unreported FCD candidate variants will reveal increased p70-S6K1 phosphorylation which is indicative of mTOR pathway hyperactivation.

Chapter 4: Methodology

4.1 Cohort inclusion:

We recruited 24 epilepsy patients (pediatric and adult), who underwent surgery to treat drug-resistant focal epilepsy and have histologically confirmed FCD on resected tissue. Ethics approval and written informed consent from each patient or parents of minors were obtained from a collaboration with the Montreal Children's Hospital, Montreal Neurological Institute and Ste Justine. For each patient, we collected (1) freshly resected brain tissue, (2) blood and/or saliva and/or buccal swabs, (3) parental blood, and (4) resected FFPE brain tissue sections, where available. Medical records describing the radiological focus, associated medical conditions, postsurgical outcome, cognition and histopathological diagnosis as well as MRI images, and neuropathology reports were obtained. Clinical information is summarized in Tables 1-3. Tissue specimens were evaluated by an experienced clinical neuropathologist prior to sequencing. Due to the variable availability of certain clinical records and pathogenic tissues based on factors that were outside of our control which include patient's personal wishes, medical exams being conducted in multiple sites, and limited access to scarce tissues, some diagnostic materials were not available for inclusion in this study.

Aim 1: Investigation of the contribution of low-level somatic mutations in FCD pathogenesis by performing ultra-deep genetic sequencing

Ultra-deep sequencing offers enhanced detection of low-level somatic mutations (≈1000-2000 read depth) relative to traditional sequencing methods such as Sanger sequencing.[77,78] We screened a total of 24 FCD brain tissue specimens for somatic mutations using a custom mTOR

pathway gene panel. Somatic variants in FCD were identified by identifying variants detected in the brain that were absent are detected at negligible levels in peripheral tissues.

4.2 Ultra-deep genetic sequencing:

DNA was extracted from fresh-frozen brain (≈25 mg), blood, saliva, and buccal swabs, where available, using QIAamp Fast DNA Tissue Kit. Target-enriched sequencing libraries were prepared and screened using a custom HaloPlex^{HS} gene panel (Agilent) containing 13 genes (*PIK3CA*, *PIK3R2*, *CCND2*, *AKT1*, *AKT2*, *AKT3*, *PTEN*, *MTOR*, *TSC1*, *TSC2*, *DEPDC5*, *NPRL2*, *NPRL3*) previously implicated in FCD pathogenesis.[18] Next, ultra-deep sequencing, using paired-end 150-bp reads, was performed on a MiSeq system (Illumina) to identify somatic variants at an AAF as low as 1% with high specificity.[6] Bioinformatic analysis was conducted using standard bioinformatics processing tools and best practices for sequence trimming, alignment to the human genome reference sequence template (GRCh37) and clinical annotation of variants. Variant calling was performed using the public DnaSeq high Coverage Pipeline (https://bitbucket.org/mugqic/mugqic_pipelines). Variant filtering criteria required the detection of ≥10 alternate strands in each sample with a base quality threshold of 30 (probability of incorrect base call is 1 in 1000) and all identified variants contained at least two distinct amplified strand pools. All variants were visualized in Integrative Genome Viewer software to ensure variants were not an artifact of amplification or processing and heterozygous coding and splice-site variants were referenced with gnomAD. Variant screening was conducted by analyzing whether variants were previously published in ClinVar (public clinical variant archive), reported in COSMIC (https://cancer.sanger.ac.uk/cosmic) or never reported in any SNP database with an AAF ≥1% (Figure 3).

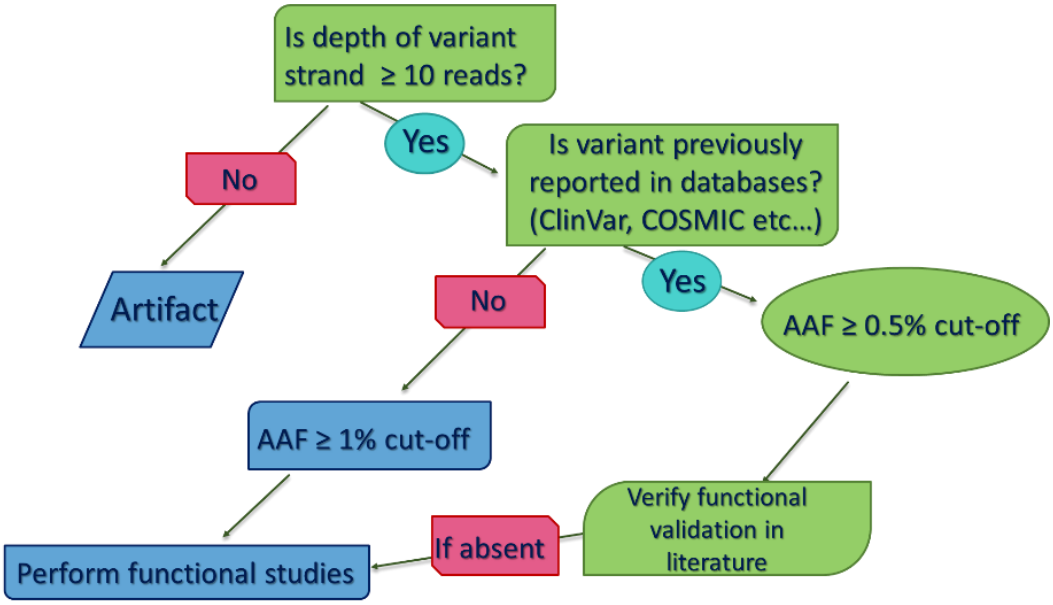

Figure 3: Flowchart illustrating the bioinformatic sequential process of variant filtering.

Following variant calling and quality control, causal or suspected causal variants were retained if they satisfied our filtering criteria. Variants which did not support these constraints were characterized as artifact.

4.3 Mutation validation and topographic mapping:

The identified variants detected with our custom panel were validated using targeted ultra-deep sequencing of FFPE brain tissue sections, fresh-frozen brain and blood and saliva using a Nextera XT DNA Preparation Kit (≈100 000 read depth). DNA was extracted from all samples using either the QIAamp DNA FFPE Tissue Kit, AllPrep DNA/RNA Mini Kit or QIAamp DNA Blood Mini Kit, respectively. For FFPE cassettes, eight serial sections of 10 µ thickness were cut from each block and processed using manufacturer's specifications. Custom intronic primers were used to target, and PCR amplify each variant region of interest. Sequencing of libraries was conducted using a MiSeq system using paired-end 150-bp reads (Illumina). Standard bioinformatics processing tools were used as previously described. Variants were determined to be somatic if absent or detected at negligible levels in peripheral tissues.

Mutation loads were calculated using the AAF formula described in section 2.6, and the allele fraction was mapped to MRI images using multiple FFPE brain tissue blocks per patient. Reconstructed FFPE brain sections using MRI images were used to correlate the topographic mutation distribution with the radiological abnormality, tissue section specific histopathological classification and postoperative outcome of each FCD patient. FCD lesion size was approximated based on the extent of the radiological abnormality, histological features detected in resected tissue and corresponding presence of mutation in each sample.

Aim 2: Functional validation of novel FCD candidate variants for their role in mTOR pathway hyperactivation using site-directed mutagenesis and in vitro transient co-transfection.

Transfection of mutant plasmid constructs in HEK293T offers a cost-effective and efficient functional assay to examine the effect of novel candidate variants on mTOR pathway hyperactivation.[79] In total, we screened 2 previously unreported FCD variants for their role in hyperphosphorylation of downstream mTOR pathway targets. p70-S6K1 hyperphosphorylation is a well-established standard readout of mTOR pathway hyperactivation. [6]

4.4 Site-directed mutagenesis:

Identified *MTOR* (NM_004958.3) variants c.7499T>A, p.Ile2500Asn from Patient 9 and c.4373_4375dupATG, p.Asp1458dup, from Patient 10 which are not yet reported in the literature were cloned into wild type (WT) pcDNA3 Flag-mTOR expressing plasmids (#26603) acquired from the Addgene repository using the QuikChange Lightning site-directed mutagenesis kit (Agilent). Bacterial transformation of variants was conducted using the Stbl3 E. coli bacteria

vehicle for plasmid amplification (Thermo Fisher). Plasmids were purified from E. coli using the Plasmid DNA Maxiprep kit (Geneaid). Subsequently, Sanger sequencing was used to verify that the desired mutation was obtained, and the remaining vector sequence was unaltered.

4.5 Transient co-transfection:

HEK293T cells (Sigma-Aldrich), grown in Dulbecco's Modified Eagle's Medium (DMEM), supplemented with Fetal Bovine Serum (FBS) were seeded into 6-well plates in standard tissue culture. Transient co-transfection using Lipofectamine 2000 (Thermo Fisher) was conducted 24 hours after seeding, with cells at 70% confluency, using 2 μg of WT or mutant mTOR and 2 μg of HA-p70-S6K1 expressing plasmids, followed by whole-cell lysis 48 hours after transfection in lysis buffer. Gel electrophoresis of lysates using 10% SDS-PAGE at 120V was run for 1.5 hours.

4.6 Western blotting:

Western blotting was performed using standard methods for transfer (60V for 2 hours in 1× transfer buffer), blocking (5% BSA for 1 hour), and primary and secondary antibody incubation. Blots were probed for HA-p70-S6K1 (transfection control), flag-mTOR (transfection control), β-actin (loading control) and p70-S6K1 hyperphosphorylation. In addition, WT mTOR was treated with 250nM Torin1 for 1 hour prior to lysing to examine the acute downstream effect of mTOR inhibitors on suppressing p70-S6K1 hyperphosphorylation. An empty vector was included as a negative control for transfection. In addition, two comparable mutant mTOR expressing plasmids known to upregulate the mTOR pathway with variants located near or at the same nucleotide position as our novel FCD candidate variants (plasmid flag-mTOR-Ile2500Phe,

similar to the variant tested in Patient 9, and plasmid flag-mTOR-Leu1460Pro, similar to the variant tested in Patient 10), were included as positive controls. Specifications for the plasmids used can be found in table S1 of the appendices. Three independent western blot repeats were performed. ImageJ, Version 1.53j, (https://imagej.nih.gov/ij/index.html), analysis was conducted for quantification of signal intensity of the bands. Statistical tests applied were one-way analysis of variance (ANOVA) followed by Dunnett's post hoc test.

Chapter 5: Research Findings

5.1 Diagnostic yield of mTOR pathway variants detected in FCD:

Fresh-frozen resected brain tissue from 24 patients (10 females, 14 males), with histologically confirmed FCDs were sequenced on a custom mTOR pathway gene panel to detect low-level somatic variants. In our cohort, 58% (14/24) of patients had causal pathogenic variants in the mTOR pathway (Figure 4). 86% (12/14) of the variants detected in our cohort were gain of function in positive regulators of the mTOR pathway, and 14% (2/14) of the variants were loss of function in negative regulators of the mTOR pathway. A summary table of the clinical features and genetic findings in each patient with an identified variant can be found in Table 1.

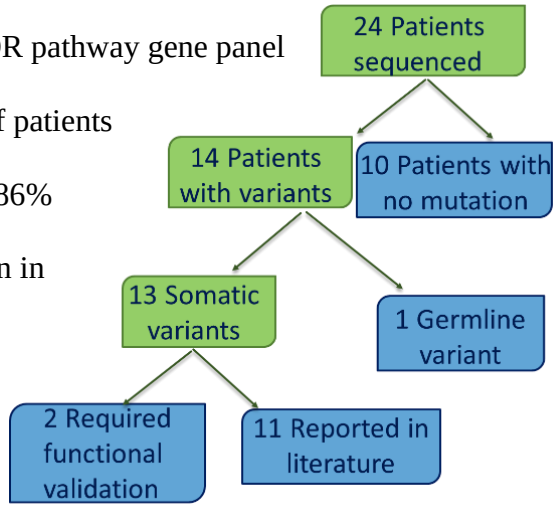

Figure 4: Overview of identified variants. mTOR pathway variants were detected in 58% of patients in our cohort.

We were unable to identify the causal pathogenic variants in 10 FCD samples. Panel negative individuals may have mTOR pathway mutations at levels which we were unable to detect, and are listed in Table 2 of the appendices. Surprisingly, 90% (9/10) of patients who were negative for mTOR pathway variants in our cohort had favourable postsurgical outcomes and did not require further surgery, suggesting that some low-level somatic variants remained undetectable with targeted panel sequencing. We were unable to identify the causal mTOR pathway variants in both patients with FCD type I on histopathology. The potential reasons for individuals who are negative on targeted panel sequencing may include, absence of mutation within the surgical sample (i.e. the variant is present in an untested neighbouring tissue section), strand depth which is below the detection threshold, a mutation located outside of the coding regions sequenced, other genes are involved that are not reported in

the literature, presence of gene deletion or duplication that cannot be detected or epigenetic factors.[18,80,]

We successfully detected somatic variants at extremely low mutation loads due to the robustness of our custom targeted gene panel. The majority of the mutations identified were in the *MTOR* gene, which comprised a total of 64% (9 /14) of the total genes detected (Figure 5). The minimum AAF retention threshold, based on best practices, applied to our cohort for variants previously reported in the literature, and variants not previously reported, is 0.5%, and 1% respectively. A summary of all variants previously reported in FCD type I and II can be found in Tables S2 and S3 of the appendices, respectively. We were able to identify causal variants at an AAF as low as 0.6%. The average age of seizure onset for patients with identified mutations is 4 years. We detected causal variants in 5 patients at an AAF below 1% indicating the importance of using a specialized custom panel with sufficiently high read depth when screening FCD tissue for somatic mTOR pathway mutations. Interestingly, one surgery was effective in alleviating seizures for a period greater than 2 years post-resection for all patients with an AAF below 1% (Table 3).

Variants were validated in blood, saliva or buccal swabs, where available, to determine whether the variant is somatic or germline. Targeted sequencing in blood and/or saliva revealed that 1 of the identified variants is germline. A loss of function mutation in *DEPDC5* (c.2802-1G>C), identified in Patient 4, was found in blood at an AAF of 50.8% with 83734/164806 variant/total strands detected. The *DEPDC5* mutation was inherited from her asymptomatic mother and a second genetic hit was not detected following additional RNA sequencing of *DEPDC5* in brain tissue. All other variants were detected at negligible levels in peripheral

tissues except for Patient 6 who has CLOVES syndrome and had their somatic mutation identified in DNA extracted from a buccal swab in the region involved with the overgrowth.

Patient (sex, current age)	Age at seizure onset	Clinical	Cognition	MRI	Histology	Seizure outcome after last surgery	Gene	Nucleotide, protein change	Allele frequency (alternate/total)		
									Brain	Blood	Saliva
1 (M, 20y)	3y	Focal epilepsy (R frontal)	Normal	R parieto-occipital and frontal FCD	FCDIIb	Seizure-free	*MTOR*	c.4447T>C p.Cys1483Arg	2.6% (38/1476)	0.02% (293/143682)	0.2% (6/30326)
2 (M, 43y)	9y	Focal epilepsy (R fronto-temporal), R HME, R OVG, Hypomelanosis of Ito	Normal IQ, Learning disability	R HME with FCD	FCDIIa	Transient decrease	*MTOR*	c.4448G>A p.Cys1483Tyr	8.5% (124/1462)	n.a.	0.27% (454/167241)
3 (M, 8y)	3y	Focal epilepsy (L frontal)	Normal IQ	L frontal FCD	FCDIIb	Seizure-free	*MTOR*	c.5930C>A p.Thr1977Lys	0.8% (32/4282)	0.06% (97/55834)	n.a.
4 (F, 18y)	1d	Focal epilepsy (R frontal)	Severe ID	R frontal FCD	FCDIIa	Decrease	*DEPDC5*	c.2802-1G>C	33.7% (635/1882)	50.8% (83734/164806)	n.a.
5 (M, 10y)	n.a.	Focal epilepsy	n.a.	Polymicrogyria	FCD	n.a.	*PIK3CA*	c.1624G>A p.Glu542Lys	12% (167/1386)	n.a.	n.a.
6 (M, 18y)	1d	CLOVES Syndrome, Infantile spasms	Global developmental delay, Severe ID	HME with R temporal FCD	FCD	Seizure-free	*PIK3CA*	c.1624G>A p.Glu542Lys	4.5% (17/382)	0.07% (24/34357)	4.85% (1681/34641)
7 (M, 8y)	18m	Focal epilepsy (R frontal)	Normal	R frontal FCD	FCDIIb	Seizure-free	*MTOR*	c.6644C>A p.Ser2215Tyr	0.9% (21/2408)	0.07% (28/40837)	n.a.
8 (F, 5y)	n.a.	Focal epilepsy	n.a.	FCD	FCDIIa	n.a.	*MTOR*	c.6644C>T p.Ser2215Phe	0.9% (15/1579)	n.a.	n.a.
9 (F, 2y)	16m	Focal epilepsy (R frontal)	n.a.	R frontal FCD	FCDIIa	Persistent	*MTOR*	c.7499T>A p.Ile2500Asn	3.5% (56/1588)	0.12% (84/69153)	n.a.
10 (F, 31y)	12y	Focal epilepsy (R posterior cingulate cortex)	Severe ID, Delayed response	R posterior FCD	FCDIIa	Transient decrease	*MTOR*	c.4373_4375dupATG p.Asp1458dup	3.1% (80/2552)	0.04% (42/99111)	0.07% (48/69090)
11 (M, 7y)	1d	Focal epilepsy (L temporal)	Global developmental delay	L HME	FCDIIa	Seizure-free	*AKT3*	c.49G>A p.Glu17Lys	4.9% (74/1508)	n.a.	n.a.
12 (M, 4y)	3m	TSC, Focal epilepsy (L fronto-temporal)	Developmental delay	L posterior FCD	FCDIIb	Seizure-free	*TSC2*	c.2356-1G>A	9.4% (306/3269)	n.a.	n.a.
13 (F, 44y)	9y	Focal epilepsy (L fronto-temporal)	Subtle learning deficits	R Anterior FCD	FCDIIa	Seizure-free	*MTOR*	c.6644C>T p.Ser2215Phe	0.7% (28/3980)	n.a.	n.a.
14 (F, 13y)	7y	Focal epilepsy (L Parietotemporal)	Normal	L supramarginal gyrus FCD	FCDIIb	Seizure-free	*MTOR*	c.5930C>A p.Thr1977Lys	0.6% (31/4985)	n.a.	n.a.

Table 1: Patients with mTOR pathway variants detected from targeted panel sequencing.

Somatic variants were present in *MTOR, PIK3CA, AKT3, TSC2* and *DEPDC5*. The average age of seizure onset for patients with identified variants is ≈4 years, with three patients experiencing seizure onset within the first day of life. The most common genes with identified variants were *MTOR* and *PIK3CA*, at 64% (9 /14), and 14% (2/14), respectively. ID= intellectual disability, GDD= global developmental delay, M= male, F= female, y= year, d= day, m= month, R= right, L= left, OVG= overgrowth, TSC= tuberous sclerosis complex, HME= Hemimegalencephaly, IQ= intelligence quotient, n.a.= not available, CLOVES= Congenital lipomatous overgrowth, vascular malformations, epidermal nevi and scoliosis/skeletal/spinal anomalies. Note: the somatic mutation identified in Patient 6 was detected from buccal swab DNA from the region involved with the overgrowth.

Patient (sex, age)	Age at seizure onset	Clinical	Cognition	MRI	Histology	Seizure outcome after last surgery
15, (F, 19y)	8y	Focal Epilepsy	Normal	R frontal parietal cortical dysplasia	FCDIIA	Seizure free
16, (M, 10y)	3y	Refractory Focal Epilepsy	Normal	L pre-central frontal lobe	FCDIIA	Seizure free
17, (F, 14y)	2y	Refractory Focal Epilepsy	Normal	R frontal lesion	FCDIIA	Seizure free
18, (F, 14y)	10y	Refractory Focal Epilepsy	Normal	R frontal superficial SMA above lesion	FCDIIA	Seizure free
19, (F, 10y)	5y	Focal Epilepsy	Normal	Temporo-parietal lobe	FCDIIB	Seizure free
20, (M, 10y)	20m	Focal Epilepsy	Severe development delay	R parieto-occipital and posterior temporal lobes	FCDIIA	No improvement
21, (M, 10y)	18m	Focal Epilepsy Landau kleffner Syndrome	Developmental delay	Relatively unremarkable, decreased size of hippocampus	FCDIA	Seizure free
22, (M, 3y)	4m	Epilepsy posterior quadrant	Developmental delay	Parietal lobe	FCDIA	Seizure free
23, (M, 60y)	20y	FCD Hippocampal Sclerosis	Normal	Temporal lobe	FCDIIA	Seizure free
24, (M, 32y)	10m	Focal Epilepsy	Normal	Temporal lobe	FCDIIA	Seizure free

Table 2: Patients without causal pathogenic variant identified

Patients 15-24 were negative on our custom mTOR pathway gene panel. The average age of seizure onset for patients without identified variants is ≈5 years, 90% (9/10) of patients had favourable post-surgical outcomes after resection. Note: two patients have FCD type I on histopathology.

Patient number	Seizure onset	Year of surgery specimen collected	Short-term Postsurgical outcome	Gene	Nucleotide, protein change	AAF	Total number of surgeries	Current epilepsy status
1	3y	2016	Seizure-free	*MTOR*	c.4447T>C, p.Cys1483Arg	AAF=2.6%	3 (2010, 2012, 2016)	Seizure-free
2	9y	2016	Seizures returned in 2017	*MTOR*	c.4448G>A, p.Cys1483Tyr	AAF=8.5%	3 (2011, 2016, 2017**)	Improved but persistent seizures
3	3y	2016	Seizure-free	*MTOR*	c.5930C>A, p.Thr1977Lys	AAF=0.8%	1 (2016)	Seizure-free
4	1d	2015	Seizure recurrence after 1 year	*DEPDC5*	c.2802-1G>C	AAF=33.7%	3 (2002, 2003, 2015*)	Persistent seizures
5	n.a.	2015	n.a.	*PIK3CA*	c.1624G>A, p.Glu542Lys	AAF=12%	n.a.	n.a.
6	1d	2017	Seizure-free	*PIK3CA*	c.1624G>A, p.Glu542Lys	AAF=4.5%	1 (2017*)	Seizure-free
7	18m	2018	Seizure-free	*MTOR*	c.6644C>A, p.Ser2215Tyr	AAF=0.9%	1 (2018)	One febrile seizure in 2019
8	n.a.	2017	n.a.	*MTOR*	c.6644C>T, p.Ser2215Phe	AAF=0.9%	n.a.	n.a.
9	16m	2018	No improvement	*MTOR*	c.7499T>A, p.Ile2500Asn	AAF=3.5%	2 (2018*)	Deceased
10	12y	2018	Transient improvement	*MTOR*	c.4373_4375dupATG, p.Asp1458dup	AAF=3.1%	2 (2018, 2019)	Seizures 1-2 times a week
11	1d	2015	Seizure-free	*AKT3*	c.49G>A, p.Glu17Lys	AAF=4.9%	1 (2018) and surgery upcoming	Infrequent seizures
12	3m	2018	n.a.	*TSC2*	c.2356-1G>A	AAF=9.4%	n.a.	n.a.
13	9y	2018	Seizure-free	*MTOR*	c.6644C>T, p.Ser2215Phe	AAF=0.7%	1	Seizure-free
14	7y	2018	Seizure free	*MTOR*	c.5930C>A, p.Thr1977Lys	AAF=0.6%	1	Seizure-free
15	8y	2016	Seizure free	--	--	--	1	Seizure free
16	3y	2018	Seizure free	--	--	--	1	Seizure free
17	2y	2018	Seizure free	--	--	--	2 (2014, 2018)	Seizure free
18	10y	2018	Seizure free	--	--	--	1	Seizure free
19	5y	2016	Seizure free	--	--	--	1	Seizure free
20	20m	2017	No improvement	--	--	--	2 (2017, 2018*)	Deceased
21	18m	2019	Seizure free	--	--	--	1	Seizure free
22	4m	2015	Seizure free	--	--	--	n.a.	Seizure free
23	20y	2019	Seizure free	--	--	--	1	Seizure free
24	10m	2019	Seizure free	--	--	--	1	Seizure free

Table 3: Epilepsy and surgical interventions.

All five patients who had an AAF below 1% were able to alleviate seizures with one surgery for a period of greater than 2 years post-resection. Four patients had a hemispherectomy and one patient had a callosotomy. Seven patients required more than one separate surgical intervention for refractory epilepsy. * hemispherectomy; **callosotomy.

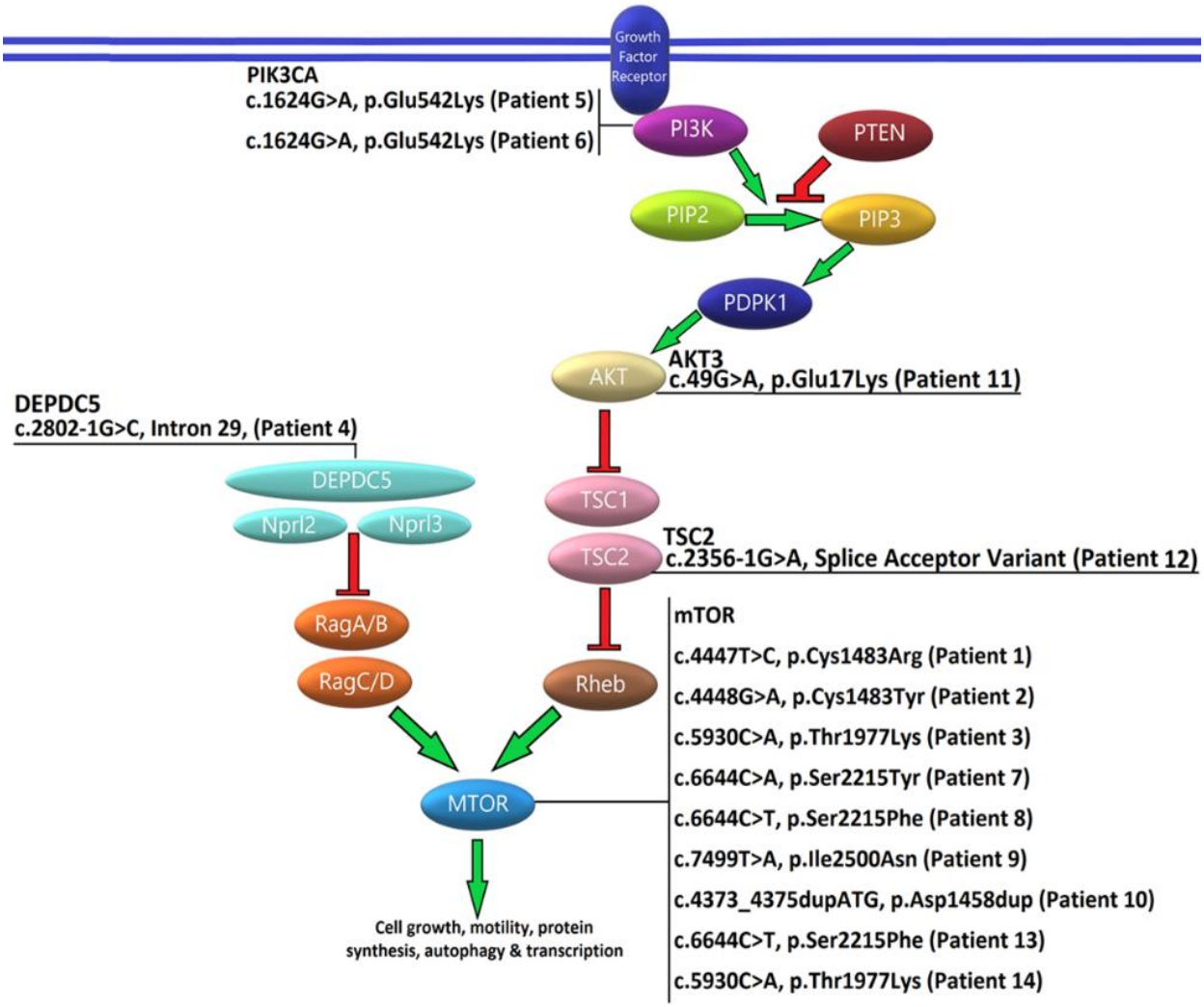

Figure 5: Schematic representation of 14 pathogenic variants detected with the corresponding patient number and location.

Variants in *MTOR*, *PIK3CA*, and *AKT3* are all somatic gain of function variants in positive regulators of the mTOR pathway. *DEPDC5* and *TSC2* are loss of function variants in negative regulators of the mTOR pathway and additional RNA sequencing of *DEPDC5* in brain tissue did not yield a second hit.

5.2 Identification of novel mTOR pathway variants in FCD:

Two variants in the *MTOR* gene (NM_004958.3), c.7499T>A, from Patient 9 and c.4373_4375dupATG, from Patient 10, are not yet reported in the literature and required functional validation.

Patient 9 was previously healthy, with normal development, and began having focal seizures at 16 months of age. She was initially controlled on Levetiracetam (Keppra), which inhibits presynaptic calcium channels.[81] At the age of 23 months she presented in refractory status epilepticus and was admitted to the ICU. Multiple antiepileptic medications, including intravenous anesthetic infusions, failed to stop her seizures. After 3 weeks, she underwent and brain biopsy which revealed FCD type IIa. Subsequently, she underwent a right hemispherectomy. She passed away at 2 years of age following 41 days admission. Targeted mTOR pathway sequencing revealed a somatic variant in *MTOR* (c.7499T>A, p.Ile2500Asn) at an AAF of 3.5% which was not previously reported in the literature. Across both fresh brain and FFPE, the variant was present at levels ranging from 0.47% to 7.6% and was detected at negligible levels in the blood, indicating that this variant is somatic.

Patient 10 is a 29-year-old female who began having seizures with a right orbitofrontal onset zone at 12 years of age. The patient had a resection of the right precuneus/posterior cingulate gyrus, and histopathology revealed FCD type IIa. Seizures improved transiently, and the patient underwent a second right parietal lobe extension surgery in 2019 with further improvement. Targeted mTOR pathway sequencing detected a somatic single amino-acid duplication in *MTOR* (c.4373_4375dupATG, p.Asp1458dup) at an AAF of 3.1% which was not previously reported in the literature. FFPE validation detected the variant present at levels

ranging from 0.12% to 1.34%. The variant was present at negligible levels in the blood and saliva indicating the variant is somatic.

5.3 Functional validation of novel variants:

Transient co-transfection of WT or mutant mTOR with HA-p70-S6K1 was performed to supplement endogenous levels of p70-S6K1 and avoid p70-S6K1 phosphorylation saturation at position threonine 389 in order to provide a highly visualizable, robust readout of each variant's effect on mTOR pathway upregulation. Two vectors, flag-mTOR-Leu1460Pro and flag-mTOR-Ile2500Phe, previously demonstrated to upregulate the mTOR pathway were included as positive controls to obtain a benchmark value for mTOR pathway upregulation. In total, six plasmid vectors were probed for p70-S6K1 phosphorylation at position threonine 389 (Figure 6).

Quantification of the signal intensity for p-p70-S6K1 obtained across the three separate western blots revealed that p-p70-S6K1 upregulation was statistically significant relative to WT for the amino acid duplication variant from Patient 10 (c.4373_4375dupATG, p.Asp1458dup) with an 86% increase in phosphorylation at position threonine 389 (significance $P \leq 0.01$), the SNP variant from Patient 9 (c.7499T>A, p.Ile2500Asn) with a 67% increase in phosphorylation at position threonine 389 (significance $P \leq 0.05$), and the known mTOR pathway upregulation plasmid (flag-mTOR-Leu1460Pro), which was purchased from Addgene with a 226% increase in phosphorylation at position threonine 389 (significance $P \leq 0.0001$). Therefore, both patient variants, c.7499T>A, and c.4373_4375dupATG demonstrated mTOR pathway upregulation in vitro, confirming they are pathogenic (Figure 7).

It should be noted that a parallel is observed in the level of p-p70-S6K1 signal detected based on variant location. Variant Leu1460Pro is located at a similar genetic region to the variant

tested in Patient 10, and both share similar levels of p70-S6K1 phosphorylation. Similarly, the location of variant Ile2500Phe is identical to the variant tested in Patient 9, and both variants also demonstrate similar levels of p70-S6K1 phosphorylation. Therefore, variants within the same region behave similarly in upregulating p-p70-S6K1, as indicated by the similarity in the strength of the p-p70-S6K1 signal detected. This suggests that these variants disrupt essential regions of the mTOR protein, leading to the observed increase in p-p70-S6K1 levels.

Although the second known upregulating mTOR pathway mutation purchased from Addgene (flag-mTOR-Ile2500Phe) has been previously shown to result in mTOR pathway upregulation[6] the values obtained in our study did not provide enough data to demonstrate statistical significance. The plasmid encoding flag-mTOR-Ile2500Phe had an overall 21% mean increase in phosphorylation at position threonine 389 relative to WT mTOR, which could be due to experimental variability or the stringent constraints of our assay. The standard error of the mean (SEM) was below 0.17 for all plasmid lanes.

Following acute administration of 250nM Torin1, the normalized mean of the treated mTOR sample decreased by 17.5% relative to WT mTOR. This result indicates that although our Torin1 treated sample appears to decrease levels of p70-S6K1 phosphorylation, a statistical determination could not be made based on the relatively low concentration and short duration of administration of Torin1. Additional studies using higher concentrations and longer incubation times would likely yield more pronounced effects.

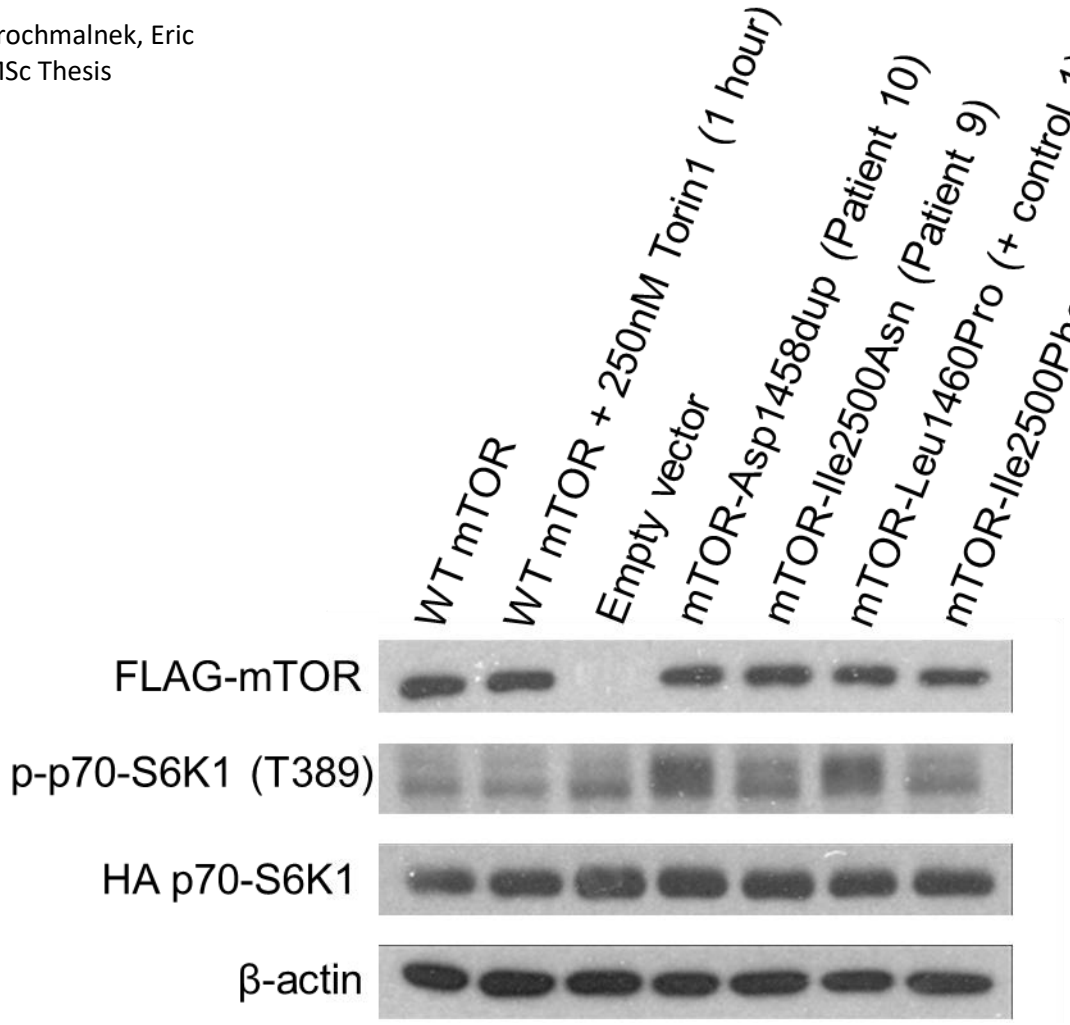

Figure 6: Functional validation of novel *MTOR* variants c.4373_4375dupATG, p.Asp1458dup and c.7499T>A, p.Ile2500Asn. The flag tagged mutant *MTOR* plasmid constructs were co-transfected with HA-p70-S6K1 in HEK293T cells to probe for hyperphosphorylation of threonine 389. Blotting for p-p70-S6 kinase at threonine 389 reveals upregulation of the mTOR pathway in both patient's variants. Interestingly, variant Asp1458dup from Patient 10 and the corresponding positive control, Leu1460Pro, both show strong mTOR pathway upregulation as indicated by elevated levels of p-p70 S6 kinase relative to variant Ile2500Asn from Patient 9 and the corresponding positive control, Ile2500Phe. From left to right, the lanes were loaded as follows; (lane 1) WT flag-mTOR vector to obtain a baseline reference measurement, (lane 2) a WT flag-mTOR vector treated with 250nM of the mTOR inhibitor Torin1 to visualize the effect of acute administration of Torin1 on surprising p70-S6K1 phosphorylation, (lane 3) an empty vector as a transfection control, (lane 4) a recombinant plasmid containing the amino acid duplication from Patient 10 (c.4373_4375dupATG, p.Asp1458dup), (lane 5) a recombinant plasmid containing the SNP variant from Patient 9 (c.7499T>A, p.Ile2500Asn), (lane 6) an upregulating mTOR pathway mutation similar to the variant found in Patient 10 (flag-mTOR-Leu1460Pro), (lane 7) an upregulating mTOR pathway mutation similar to the variant tested in Patient 9 (flag-mTOR-Ile2500Phe). HA and Flag tags indicate equal co-transfection of p70-S6K1 and mTOR plasmids respectively. B-actin is a cell lysate loading control. Figure produced in collaboration with the Sonenberg Lab.

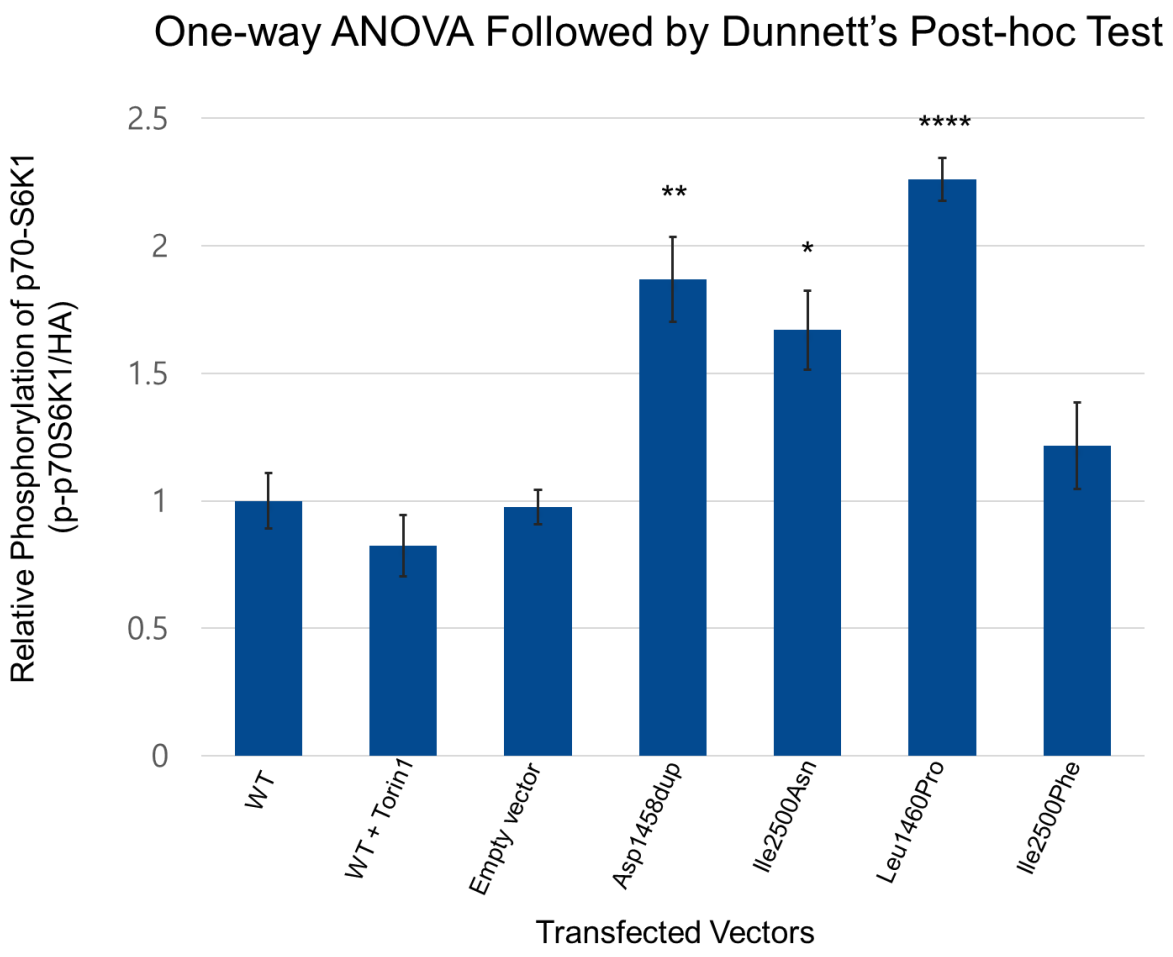

Figure 7: Statistical analysis of the relative levels of p-p70 S6 kinase signal intensity.

A statistically significant increase in levels of p70-S6K1 phosphorylation relative to WT was observed for variants, p.Asp1458dup and p.Ile2500Asn from patients 9 and 10, as well as a known upregulating mTOR pathway mutation (flag-mTOR-Leu1460Pro) located at a similar genetic region to the variant found in Patient 10. The increased p70-S6K1 phosphorylation levels detected demonstrate mTOR pathway upregulation, confirming variants from patients 9 and 10 are pathogenic. Statistical values: *= $P \leq 0.05$, **= $P \leq 0.01$, ****= $P \leq 0.0001$. Figure produced in collaboration with the Sonenberg Lab.

5.4 Topographic distribution of mutation load:

Multiple FFPE brain tissue sections, when available, were screened using the Nextera XT DNA library preparation kit and mapped to MRI to correlate with radiological and histopathological abnormalities. The MRI maps illustrate a sampling of the mutation load distribution at different regions throughout the resected brain and indicate the rate at which variant levels fluctuate across different distances, brain regions, and patients.

The topographic reconstruction of FFPE tissue blocks from each FCD revealed a correlation between the mutation load distribution, MRI lesion size and histopathological abnormalities. For example, four consecutive FFPE tissue blocks from Patient 5 were sequenced from the right temporal lobe displaying extensive polymicrogyria (Figure 8). In FFPE brain tissue, the mutation load ranged from an AAF of 5.06% to 22.69%. The FFPE mutation load varied translationally with brain location where the highest AAF was observed in the left-most FFPE block and progressively decreased with each consecutive slice by an average AAF of 5.88%. The decrease in AAF between sections from left to right was 2.28%, 3.30%, and 12.05% respectively, suggesting that the mutation load sharply drops off toward the perimeter of the FCD. In fresh-frozen brain tissue, the mutation load AAF was 17.63%, which is within the range detected on FFPE.

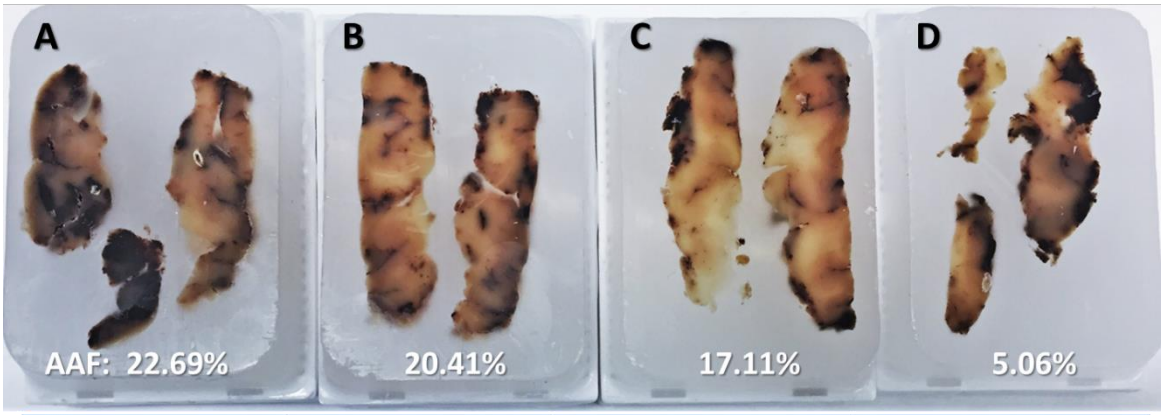

Specimen	Location	AAF Percentage	Histopathology
Fresh-frozen Brain	Frontal lobe	17.63%	Polymicrogyria
A) FFPE	Right temporal lobe	22.69%	Polymicrogyria
B) FFPE	Right temporal lobe	20.41%	Polymicrogyria
C) FFPE	Right temporal lobe	17.11%	Polymicrogyria
D) FFPE	Right temporal lobe	5.06%	Polymicrogyria

Figure 8: Serial FFPE brain tissue blocks from the right temporal lobe of Patient 5. Mutation distribution varies across the translational plane of the resection, with the most lateral and medial regions containing the highest and lowest AAF, respectively.

Specific examples of topographic FFPE MRI maps from our cohort are provided below with corresponding specimen-specific histopathological classifications:

Patient 3:

At the center of the FCD from Patient 3, the AAF detected in FFPE varied from 3.1-3.4% and contained frank FCD characteristic histologic features (Figure 9). In FFPE tissue, genetically clear or near clear resection borders were achieved with an AAF at the resection perimeter of 0.01-0.02% and the absence of distinguishing FCD features. Note that this patient has been seizure-free since his surgery. In fresh brain tissue, the mutation load AAF was 0.61% which is

within the range detected on FFPE. Patient 3 remains seizure-free following resection in 2016. Sequencing cellular surgical fluid from the Cavitron Ultrasonic Surgical Aspirator (CUSA) bag revealed an AAF of 2.5%, which provides a sampling of the mutation presence. Combining histopathological, genetic and radiological data indicates that this was a relatively small lesion with a well-defined histologically and genetically abnormal center.

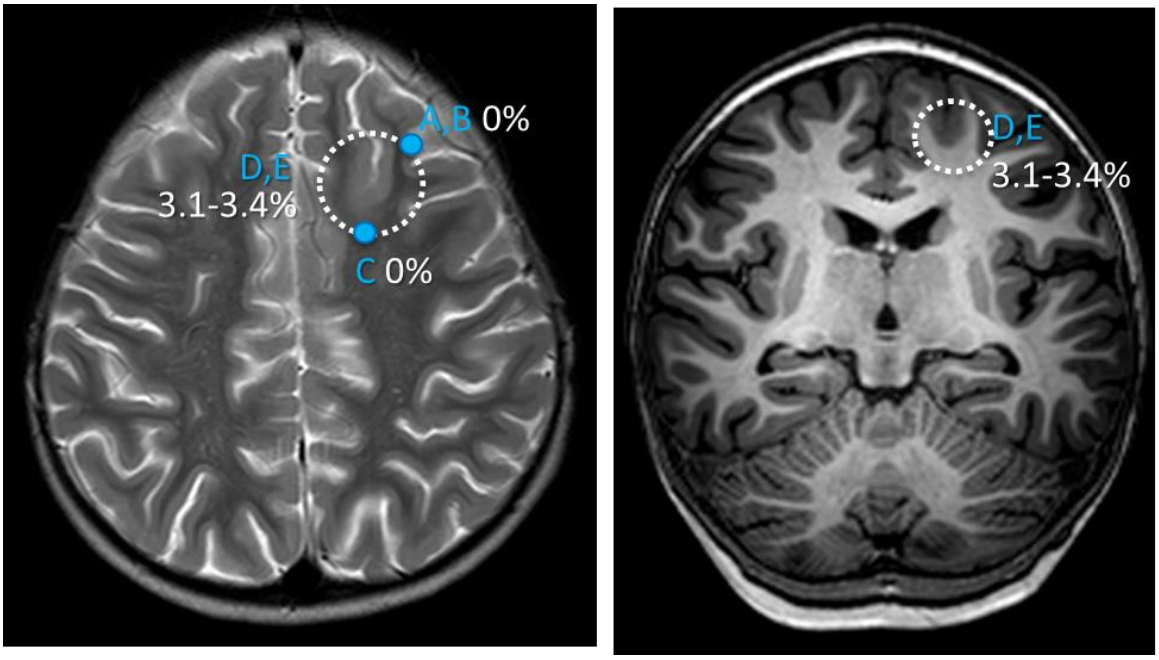

Specimen	Location	AAF Percentage	Histopathology
Fresh brain	Left bifrontal	0.61%	FCD type IIb
Blood	Systemic	0.06%	n.a.
A) FFPE	Left frontal, anterior	0.02%	FCD type IIb
B) FFPE	Left frontal lateral border	0.01%	Occasional dysmorphic neurons, no balloon cells
C) FFPE	Left frontal posterior border	0.05%	Occasional dysmorphic neurons or balloon cells
D) FFPE	Left frontal base of abnormal sulcus	3.35%	FCD type IIb
E) FFPE	Left frontal base of sulcus	3.09%	FCD type IIb
FFPE	Cusa aspirate	2.50%	FCD type IIb

Figure 9: MRI of Patient 3, in transverse and frontal planes of FCD type IIb lesion.

The resection border is identified by a white dotted circle. The patient remains seizure-free since 2016-04-06. The resection location map is labelled alphabetically. Histopathologic diagnosis correlates with mutation load, where sections with more distinct FCD features contained a higher AAF. Figure created with the help of Dr. Andrea Accogli.

Patient 9:

In Patient 9, topographic FFPE mutation mapping across both surgeries revealed the somatic mutation present at levels from 0.47% to 6.16% (Figure 10). The range of AAFs detected between the first (blue) and second (green) surgery remained largely over the same range at 1.29% - 5.37%, for the first surgery and 0.47% - 6.16% for the second surgery. A slight increase in AAF at the upper end of the range was observed with the second surgery, however, the resection also encompassed a larger brain region. In fresh brain tissue, the mutation load increased from an AAF of 4.38% detected at the first surgery to an AAF of 7.56% detected at the second surgery. Overall, the size of the lesion appears widespread over the right hemisphere where the AAF distribution throughout the lesion is highest laterally and posteriorly. Additionally, the histopathology report indicated frank FCD characteristic histologic features in widespread locations throughout the resected brain in both surgeries, with all sections in the first surgery containing frank FCD characteristic histologic features. Seizures were persistent following resection, and, unfortunately, the patient passed away with severe catastrophic epilepsy.

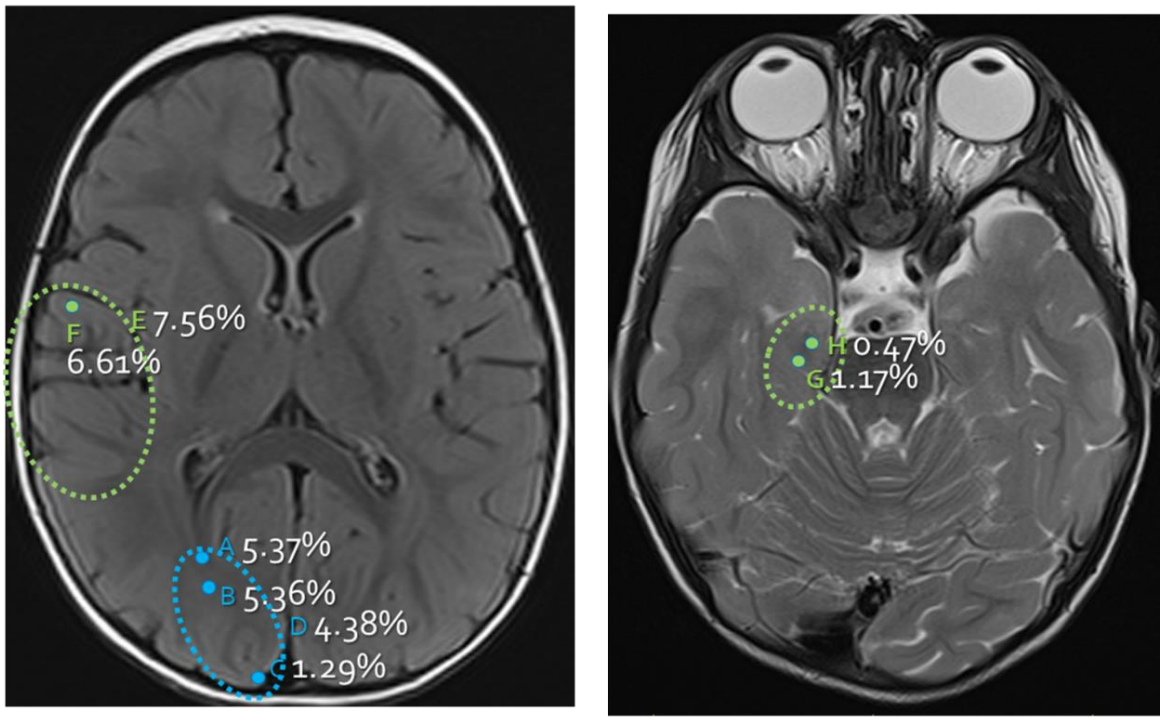

First surgery

Specimen	Location	AAF Percentage	Histopathology
Blood	Systemic	0.12%	n.a.
A) FFPE	R occipital epileptogenic	5.37%	FCD type IIa
B) FFPE	R medial occipital	5.36%	FCD type IIa
C) FFPE	R occipital pole	1.29%	FCD type IIa
FFPE	Cavitron aspirate	3.98%	FCD type IIa
D) Fresh-frozen Brain	R medial occipital lobe	4.38%	FCD type IIa

Second surgery

Specimen	Location	AAF Percentage	Histopathology
E) Fresh-frozen Brain	R anterior temporal lobe	7.56%	FCD type IIa
F) FFPE	R anterior temporal lobe	6.16%	FCD type IIa
G) FFPE	Parahippocampal gyrus	1.17%	Dysmorphic neurons
H) FFPE	Anterior temporal hippocampus	0.47%	No dysmorphic neurons
FFPE	R inferior parietal lobe	1.24%	Rare dysmorphic neurons

Figure 10: MRI of Patient 9 in a transverse plane with FCD type IIa on histology. The first surgical resection appears in blue and the second resection appears in green. The patient had catastrophic epilepsy and passed away at 2 years of age. The resection location is labelled alphabetically. Histopathologic diagnosis correlates with mutation load, where sections with more distinct FCD features contained a higher AAF.

Patient 10:

Patient 10 underwent a resection of the right parietal lobe and experienced a transient decrease in seizures following surgery. A topographic map containing pre- and postoperative MRI images was constructed (Figure 11). The highest AAF values were detected from the anterior portion of the resection (0.45% to 1.34%) and also received the most distinct histopathological hallmark classification of frank FCD type IIa. Posteriorly, the histopathological examination described only dysmorphic neurons and the corresponding AAF detected ranged from 0.06% to 0.12%. Patient 10 underwent a subsequent surgery in June 2019 with some additional improvement, suggesting that the borders of the previous surgery were not free of histological FCD features and genetic mutation. Combining histopathological, genetic and radiological data indicates that the histopathologic diagnosis correlates with mutation load, where anterior sections with more distinct FCD features contained a higher AAF.

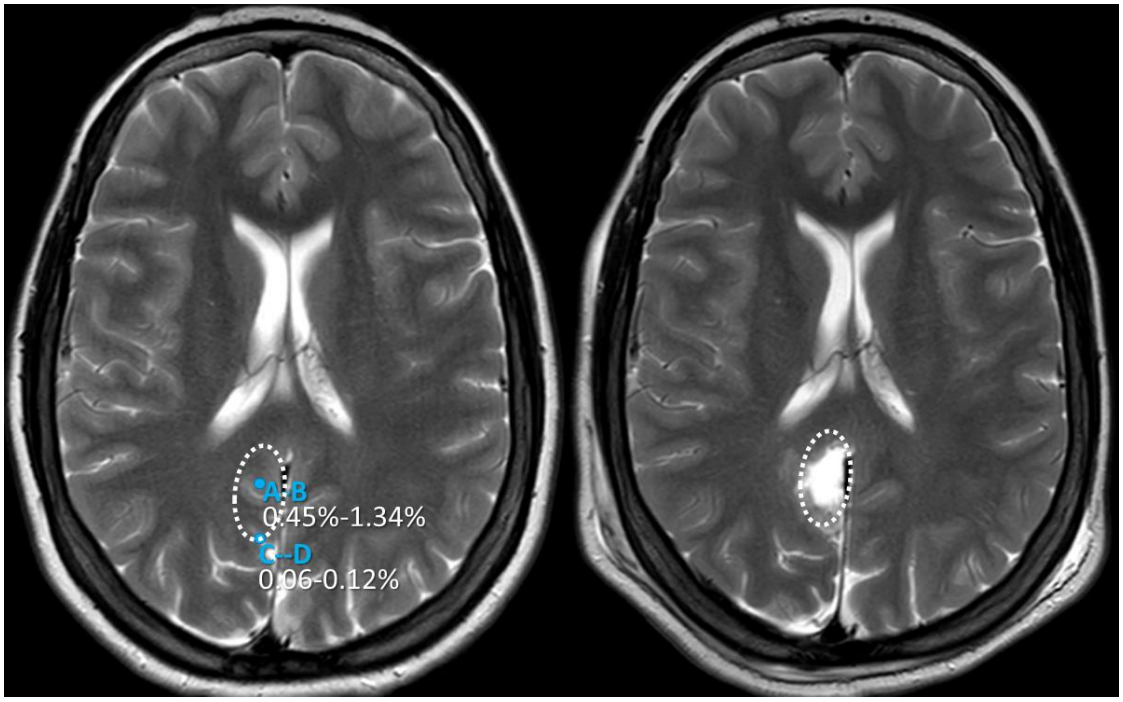

Specimen	Location	AAF Percentage	Histopathology
Blood	Systemic	0.04%	n.a.
Saliva	Oral cavity	0.07%	n.a.
A) Fresh Brain	R parietal lobe	1.34%	FCD IIA
C) Fresh Brain	Corridor section	0.06%	n.a.
D) FFPE	Corridor	0.12%	Dysmorphic neurons
B) FFPE	Lesion	0.45%	FCD IIA
FFPE	Cavitron aspirate	0.07%	n.a.

Figure 11: Pre- and postoperative MRI of Patient 10 in a transverse plane with FCD type IIa on histology.

The resection border is identified by a white dotted circle. The patient experienced a transient decrease in seizures and then underwent a subsequent surgery in June 2019 with some improvement. The resection location map is labelled alphabetically. Histopathologic diagnosis correlates with mutation load, where sections with more distinct FCD features contained a higher AAF.

Patient 7:

In Patient 7, AAF detected at the FCD center was 2.1% in FFPE and correlated with the most distinct histopathological classification of FCD type IIb (Figure 12). Around the perimeter of the lesion, the AAF tapers off radially and ranged from 0.01% - 0.1% with no dysmorphic neurons or other distinguishing FCD features reported, demonstrating genetically clear or near clear resection borders. Patient 7 remains seizure-free following resection in 2018. Combining histopathological, genetic and radiologic data indicates that this was a relatively small lesion with a well-defined histologically and genetically abnormal center. Patients 3 and 7 share many similarities in terms of histopathological and genetic mutation distribution and postsurgical outcome.

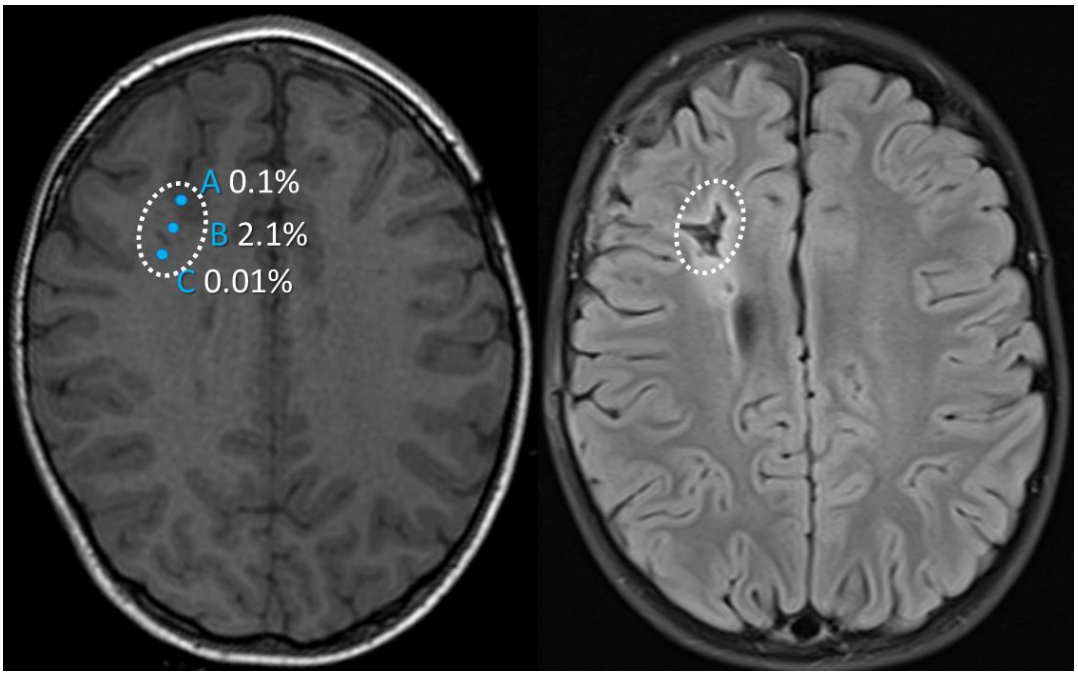

Specimen	Location	AAF Percentage	Histopathology
Blood	Systemic	0.07%	n.a.
Fresh Brain	Frontal lobe	1.89%	n.a.
A) FFPE	R frontal lobe anterior	0.1%	No dysmorphic neurons
B) FFPE	R frontal lobe medial	2.1%	FCD IIB
C) FFPE	R frontal lobe posterior	0.01%	No dysmorphic neurons
FFPE	Cavitron	0.04%	FCD IIB

Figure 12: Pre- and postoperative MRI of Patient 7 in a transverse plane with FCD type IIb on histology. The resection border is identified by a white dotted circle. The patient remains seizure-free since 2018-05-16. The resection location map is labelled alphabetically. Histopathologic diagnosis correlates with mutation load, where sections with more distinct FCD features contained a higher AAF. The highest AAF is found at the lesion center and tapers off radially.

Overall, topographic mapping of the identified mutation load with MRI from each FCD revealed that the mutation load distribution correlated with MRI lesion size and histopathological abnormalities, where favourable postsurgical outcomes were associated with clear or near clear resection borders.

5.5 Targeted bulk DNA and RNA sequencing in FCD tissue:

Mutation detection using the AllPrep parallel DNA and RNA coextraction kit on the same bulk FCD tissue section yielded surprising results. Approximately a 2-5 fold upregulation of the identified mutation was detected in targeted sequenced of cDNA relative to DNA within the same tissue (Table 4) which suggests preferential expression or retention of the mutant allele. For example, in FCD IIa sample MS-582.01, obtained from the right medial occipital lobe, the AAF of the identified mutation was detected at approximately 4.5X greater levels in RNA relative to DNA. The mechanism underlying this elevated level of mutant RNA detected remains unknown but may suggest a positive feedback loop is at play in FCD pathogenesis. In addition, mutations at upregulated levels in RNA relative to DNA may offer enhanced mutation detection capabilities with RNA sequencing, which would be especially useful for identifying mutations that are difficult to detect with conventional DNA detection methods. Further studies examining the effect of FCD mutations on RNA are recommended to elucidate the driver of this increased mutation presence.

Sample Number	Histology	Sample Comments	Mutation Detected	DNA AllPrep AAF (%)	cDNA AllPrep AAF (%)	cDNA/DNA
MS-590.01	FCDIIA	Pathogenic cingulate cortex	MTOR p.Asp1458dup	2.2	3.9	1.77
MS-590.01	FCDIIA	Nonpathogenic cingulate cortex	MTOR p.Asp1458dup	0	0	n/a
MS-85.01	FCDIIB	Sample close to onset zone	MTOR p.Cys1483Arg	7.3	23	3.15
MS-114.01	HME	Right frontotemporal parietal	MTOR p.Cys1483Tyr	9.5	38	4.00
MS-45.01	FCD IIB	Left bifrontal lobe	MTOR p.Thr1977Lys	0.68	2.6	3.82
MS-589.01	FCD IIB	Frontal lobe	MTOR p.Ser2215Tyr	2.6	5.0	1.92
MS-604.01	FCD IIA	n/a	MTOR p.Ser2215Phe	4.9	10	2.04
MS-582.01	FCD IIA	Right medial occipital lobe	MTOR p.Ile2500Asn	3.7	17	4.59
MS-582.01	FCD IIA	Anterior temporal lobe	MTOR p.Ile2500Asn	7.2	33	4.58
MS-603.01	PMG/FCD	Frontal lobe	PIK3CA p.Glu542Lys	16	30	1.88
MS-274.01	HME	Temporal pole	PIK3CA p.Glu545Lys	2.8	8.7	3.11
MS-274.01	HME	Lateral temporal lobe	PIK3CA p.Glu545Lys	1.6	2.4	1.50
MS-274.01	HME	Hippocampus	PIK3CA p.Glu545Lys	2.9	3.4	1.17
MS-274.01	HME	Frontal white matter	PIK3CA p.Glu545Lys	12	11	0.92
MS-274.01	HME	Operculum insula	PIK3CA p.Glu545Lys	32	47	1.47
MS-274.01	HME	Left frontal lobe	PIK3CA p.Glu545Lys	23	42	1.83
MS-9.01	FCD IIA	Temporal Lobe	AKT3 p.Glu17Lys	5.8	0	n/a
MS-9.01	PMG/FCD IIA	Cavitron contents	AKT3 p.Glu17Lys	1.2	0	n/a

Table 4: FCD mutation presence in DNA and cDNA libraries.

Targeted sequencing of bulk parallel extracted DNA and RNA from the same tissue section revealed approximately a 2-5-fold mutation increase detected in cDNA relative to DNA in the majority of surgical brain tissue specimens.

Chapter 6: Discussion

6.1 Enhanced detection of somatic variants:

The diagnostic yield of patients with causal pathogenic mTOR pathway variants detected in our cohort of 58% (14/24) is higher than reported in the literature due to the ability of targeted ultra-deep next-generation sequencing to detect low-level somatic variants which were previously undetectable with standard methods and the use of fresh pathological tissue specimens located at the suspected center of the FCD abnormality. Our recent finding that somatic mTOR pathway variants are expressed at a higher proportion in RNA relative to DNA across multiple samples in our cohort suggests that new diagnostic strategies for FCD may be on the horizon due to the enhanced potential to detect the upregulated mutation in RNA. Further studies examining the diagnostic efficiency of targeted RNA sequencing relative to targeted DNA sequencing may reveal a superior method of detecting low-level somatic variants due to the increased variant strand depth detected.

6.2 Genetic and histopathological correlation of FCDs:

Topographic FFPE mutation load mapping shows that some FCDs exhibit a sharp decrease in mutation load toward the border of the lesion and resections with genetically clear or near clear borders result in favourable seizure outcomes. Additionally, the AAF appeared to correlate with FCD size and histological severity. For example, in Figure 9 the highest AAF detected was 3.4% and resulted in a small lesion on MRI. However, in Figure 10 the highest AAF detected was 7.6%, and resulted in a widespread lesion encompassing a large portion of the right hemisphere. Regions with distinct FCD features on histopathology correlated with high AAF, and regions with mild or no histologic FCD features correlated with negligible or

undetectable mutation loads. No distinction in AAF was observed between FCD type IIa and type IIb.

Additionally, patients with the lowest AAFs detected had the most favourable postsurgical outcomes. Patients with well-defined focal lesions with genetically and histopathologically clear or near clear borders on topographic maps such as patients 3 and 7 had more favourable postsurgical outcomes relative to patients 5, 9 and 10. Moreover, since variant-detection likelihood increases with a greater pathological cell density[6], some panel negative patients with favourable postsurgical outcomes may have had very few pathogenic cells in their lesion. In our cohort, approximately 58% (7/12) of mutation-positive patients experienced seizure freedom post-resection for a period of greater than 2 years. However, 90% (9/10) panel negative patients experienced seizure freedom post-resection for a period of greater than 2 years, further suggesting that variants present at low AAFs correlate with the more favourable postsurgical outcomes.

6.3 Mutation prevalence at specific genetic hotspots:

Many mutations identified in our cohort are recurrent. The identification of recurrent mutations in FCD may aid in the development of hotspot testing, which is performed in many cancer types[82] and involves screening for unique, identified gene alterations that are correlated with effective targeted therapy, to rapidly screen FCD patients in the clinic. Mutation hotspots are defined as nucleotide regions within a gene that are more prone to mutation. Characteristics such as sequence specificity may increase the rate of error in repair and replication machinery or promote interaction with mutagens to result in hotspot regions. For example, homonucleotide runs, direct and inverted repeats, CG dinucleotides and microsatellite repeats can result in

misalignment or act over a significant distance and are often prone to high-frequency mutational events.[83] Recurrent mutations in FCD impact specific protein domains that are essential to the protein's structure and/or function to result in aberrant mTOR pathway hyperactivation and produce detectable FCD phenotypic characteristics.[6]

Several mutations identified in our cohort disrupt the same amino acid location in mTOR as observed in patients 7, 8 and 13 with mutations located at c.6644C>A p.Ser2215Tyr, c.6644C>T p.Ser2215Phe, c.6644C>T p.Ser2215Phe, respectively. All three patients had an AAF below 1% and experienced favourable postsurgical outcomes following surgery. The missense gain-of-function hotspot mutation at amino acid 2215 is situated within the kinase domain of mTOR (Figure 13).[84] Amino acid 2215 is located just outside the kα3 helix, which is located at the active site of the mTOR kinase and is likely an essential region involved in phosphorylation.[85] In PI3K, patients 5 and 6 in our cohort both have identical amino acid changes at the mutation hotspot c.1624G>A, p.Glu542Lys, which are frequently observed in tumours. The mutation disrupts an inhibitory charge–charge interaction with the p85α regulatory subunit by affecting the catalytic region of the PI3K helical domain (Figure 14).[86]

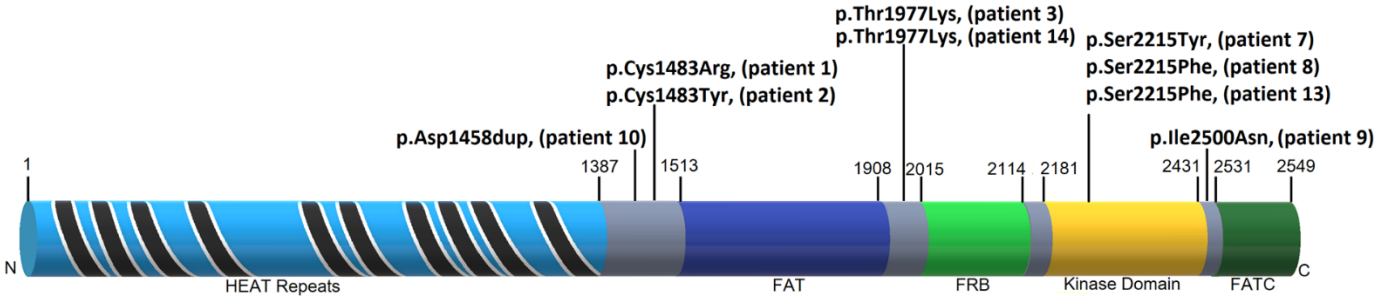

Figure 13: mTOR protein mutation mapping.

mTOR contains multiple domains which include 20 tandem HEAT repeats that provide protein-protein interactions with the mTOR regulatory proteins Raptor and Rictor, the FAT modulatory domain, the FKBP12-rapamycin binding domain (FRB), the serine/threonine kinase domain and the FATC modulatory domain.[84] Three patients in our cohort had hotspot mutations at amino acid location 2215.

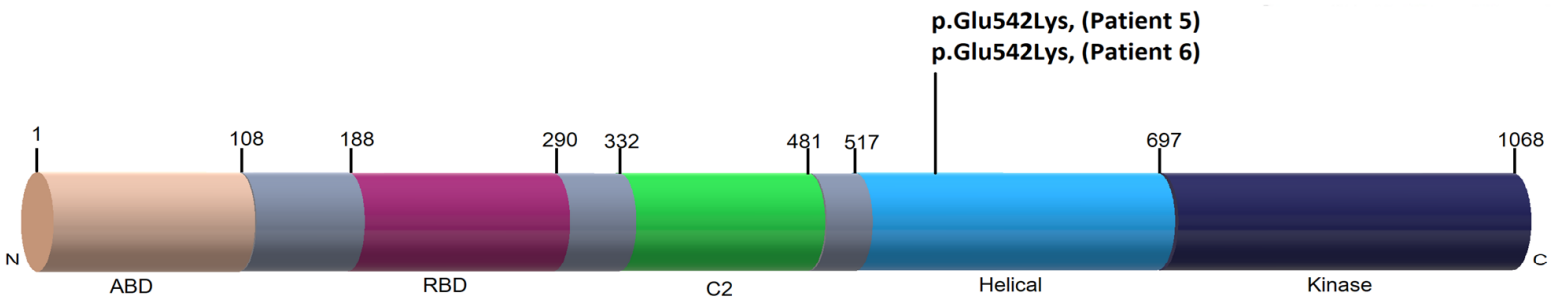

Figure 14: PI3K protein mutation mapping.

PI3K contains the following domains, an N-terminal adaptor-binding domain (ABD), a Ras-binding domain (RBD), a membrane-binding domain (C2), and helical and kinase catalytic domains.[86] Two patients in our cohort had hotspot mutations at amino acid location 542.

6.4 Protein domain mapping of novel causal variants:

Two novel variants c.7499T>A, p.Ile2500Asn, from Patient 9 and c.4373_4375dupATG, p.Asp1458dup, from Patient 10 affect different regions of mTOR. Variant c.7499T>A, p.Ile2500Asn is the most C-terminally located variant detected in our cohort and is between the kinase and FATC domains, which are responsible for the phosphorylation of downstream effectors and mTOR modulation, respectively (Figure 13). Therefore, this variant may enhance the activity of the kinase domain by providing a more favourable interaction site to promote phosphorylation, leading to downstream hyperphosphorylation and subsequent mTOR pathway upregulation. The proximity of this variant to the kinase domain increases the possibility that changes to the protein's natural secondary, tertiary or quaternary structure would impact the function of the nearby kinase. Additionally, it is also possible that the variant affects binding of essential regulatory molecules to the FATC modulatory domain, which could also lead to upregulation of the mTOR pathway.

Variant c.4373_4375dupATG, p.Asp1458dup is the most N-terminally located variant detected in our cohort and is situated between the HEAT repeats that provide protein-protein interactions with mTOR regulatory proteins and FAT modulatory domain (Figure 13). Thus, it is possible that this variant disrupts protein tertiary or quaternary structure and subsequently affects binding of essential regulatory molecules, leading to substantial upregulation of the mTOR pathway. In our functional studies, variants occurring between the HEAT repeats and FAT domain had the most pronounced effect on phosphorylation of p70-S6K1. Of note, the variants detected in Patients 1 (c.4447T>C, p.Cys1483Arg) and 2 (c.4448G>A, p.Cys1483Tyr) are also located between the HEAT repeat and FAT domains, and resulted in highly persistent seizures following surgery, with both patients 1 and 2 requiring three separate surgical interventions to alleviate seizures. Similarly, persistent seizures following surgery were observed in Patient 9, who had two surgical interventions and passed away, and Patient 10, who underwent a second surgery in 2019 and currently experiences persistent seizures once or twice a week. Further studies are needed using 3D protein X-ray crystallography to examine the extent of the protein domain-specific impact of variants on the natural 3D conformation of mTOR. In addition, immunoprecipitation assays could indicate whether these variants disrupt interaction with key mTOR complex 1/2 regulators.

6.5 Level of mTOR pathway hyperactivity on FCD pathophysiology:

Comparing the p70-S6K1 phosphorylation differences observed in our in vivo studies demonstrates that the level of mTOR pathway upregulation can vary considerably between variants. Variant specific effects on mTOR pathway upregulation levels may also play an important role in contributing to the pathogenicity of FCDs by producing variability in the disruption of the neuronal microenvironment. For example, following two separate surgical

interventions, Patient 10 currently experiences persistent seizures as often as twice a week and had a high level of mTOR pathway upregulation observed in functional studies. Therefore, in addition to mutation frequency and spatial distribution, variants disrupting specific mTOR pathway protein domains may have varying consequences on impacting neuronal microenvironment and releasable factor homeostasis. Further studies are required to examine whether variant-specific differences on mTOR pathway upregulation correlate with clinical assessments to determine whether patients would benefit from personalized medicine strategies based on the level of mTOR pathway upregulation observed.

6.6 Germline variants in FCD:

As expected, Patient 4, who has the highest mutation load on our custom panel (AAF of 33.7%) detected in *DEPDC5* (c.2802-1G>C), was found to have an AAF of 50.8% in peripheral blood using a Nextera XT DNA library preparation kit, indicating that the variant is germline, and can be detected in blood-derived DNA. Although a second genetic hit in *DEPDC5* was not detected, there is a recent emergence of the potential for mTOR pathway mutations to have an additive or combinatorial effect on mTOR pathway upregulation.[87] It remains possible that another variant that is not on our panel is acting in concert with the *DEPDC5* variant to upregulate the mTOR pathway or the strength of this mutation on mTOR pathway upregulation may be sufficient to observe a phenotype. Further studies on the strength of individual variants on mTOR pathway upregulation in animal models are recommended to determine how the mutation affects the manifestation of FCD pathophysiology.

6.7 FCD as a heterogeneous focal lesion:

Many pathogenic aspects of FCDs remain unknown. For example, given the mTOR pathway's widespread activity in cell growth, survival and proliferation it is also commonly associated with roles in tumour cell biology.[88] In general, most tissues of the body have rapidly dividing cells, and a sporadic de novo somatic pathogenic variant in the mTOR pathway can give rise to cancer by promoting cell proliferation and metabolism that can contribute to tumorigenesis.[28] However, only a small number of neurons will continue to be regenerated throughout our lives, with the majority of neurons being incapable of dividing to form new neuronal populations.[89] It remains unknown how few mosaic cells within a heterogeneous lesion can give rise to severe forms of epilepsy. The combination of somatic mutations with the limited proliferative capability of nervous system tissues may help explain the unique lesion morphology observed in FMCD. Therefore, in addition to cytoarchitectural disruption, factors such as non-cell-autonomous effects, inflammation and miRNAs likely play a key role in the manifestation of seizures in FMCD.[7] Further studies are needed to examine the effects of somatic mutations at the individual cellular level to better understand the pathophysiological mechanisms underpinning FCD.

6.8 Modulation of the mTOR pathway:

There is growing interest in identifying treatments for mTORopathies associated with FMCD and our study paves the way for FCD clinical trials involving mTOR inhibitors, especially in cases where mosaic variants can be detected in peripheral samples (blood, cerebrospinal fluid or buccal swabs), such as in TSC cases.[65] In humans, rapamycin therapy has been shown to exhibit significant positive effects on epileptic seizures in cases of TSC over a

period of 2 years.[45] In addition, an HME patient experienced a >50% reduction in seizures following rapamycin treatment.[64] To date, no clinical trials in humans have been published on the effects of rapamycin or other mTOR inhibitors on FCD. Identifying drugs to treat FCD is especially pressing as patients can undergo catastrophic morbidity if left untreated.[2] Our study provides the foundation for clinical trials to test the efficacy of rapamycin in seizure management. Personalized mutation detection can indicate whether the binding site of a particular drug is altered or determine the strength of mTOR pathway upregulation, which could further aid in pharmacological management by identifying which mTOR inhibitors bind optimally to the mutated protein or guiding the quantity of pharmacologic agent required to attenuate the mTOR pathway.

6.9 FCD type I emerging as a distinct genetic entity:

Recently, FCD type I was described as part of a distinct genetic entity, whereas the mTOR pathway is associated primarily with FCD type II. Presently, pathogenic variants in *SLC35A2*, a gene involved in the N-glycosylation pathway, have been shown to account for 29% of mild malformations of cortical development/FCD type I cases.[6] Two patients in our cohort had FCD type I on histopathology and both were negative for mTOR pathway mutations (Table 2). Taken together, our results are consistent with this recent genetic FCD subtype divergence in the literature, and an ILAE update to the FCD classification system is in progress.[26] The diagnostic yield of mTOR pathway variants in patients with FCD type II on histopathology in our cohort is 64% (14/22), with a somatic variant AAF range of 0.6-12% in fresh tissue. A further breakdown by histopathological subcategory shows that mTOR pathway variants comprise 50% (7/14) of FCD type IIa, with a somatic variant AAF range of 0.7-8.5% in fresh

tissue and 83% (5/6) of FCD type IIb patients in our cohort, with a somatic variant AAF range of 0.6-9.4% in fresh tissue, respectively. This discrepancy in diagnostic yield between subtypes may indicate that additional mechanisms are at play in the pathophysiology of FCD type IIa.

6.10 Future directions:

For samples that remain unexplained, we could further assess mTOR pathway hyperactivation immunohistochemically and check for altered gene-splicing using RNA sequencing.[90] Additionally, due to the versatility variant detection with our custom panel, rescreening negative patients with an updated gene panel that includes newly reported genes implicated in FCD pathogenesis such as *IRS-1*,[87] *SLC35A2*,[6] *STRADα*,[18] *RHEB*,[49] *TBC1D7*[18] and *RPS6*[48] may further enhance detection of variants. Moreover, DNA methylation and miRNAs are two emerging epigenetic mechanisms that may contribute to FCD pathogenesis in our cohort that would be undetectable with targeted genetic sequencing.[18] Therefore, methylome analysis and miRNA sequencing could provide useful insight into the downstream effects of epigenetic mechanisms and their role in FCD pathogenesis.

Emerging highly accurate computer-assisted technology for MRI presurgical assessment such as surface-based morphometry analysis to assist with automated identification of the precise FCD location may similarly benefit from the integration of molecular diagnostic information together with surface-based features for improved lesion detection in subsequent surgeries. Presently, this surface-based morphometric analysis is based primarily on an estimation of the shape of cortical surfaces and includes surface-based metrics such as cortical thickness, pial surface area, cortical curvature data.[91] However, training these computer-generated algorithms to correlate histopathological abnormalities with patient-specific mutation load input information,

variant strength and postsurgical outcomes may further enhance the identification of distinct FCD structural profiles on MRI.[72] Including a database of genetic-centred information into MRI diagnostic machine learning technology for pre-evaluation may aid in the development of new objective, time-efficient tools to plan efficient surgeries for patients who undergo multiple resections and may ultimately further improve post-surgical outcomes.[91]

6.11 Summary:

Screening for somatic mutations in the mTOR pathway using a custom panel is feasible, results in a high yield, and detects variants with an AAF below 1%. Overall, causal pathogenic variants were detected in 14 out of 24 individuals. In this study, we were successfully able to detect somatic variants with an AAF as low as 0.6%, with all patients with AAFs below 1% achieving seizure freedom for a period greater than 2 years post-resection. Moreover, topographic mapping revealed the convergence between radiological, histopathological and genetic elements of FCD pathogenesis. In addition, functional studies revealed that both novel FCD variants, c.7499T>A, and c.4373_4375dupATG significantly increase p70-S6K1 phosphorylation at position threonine 389 in vitro. Furthermore, elevated expression or retention of pathogenic causal mTOR pathway variants in RNA may aid in the enhanced detection of FCD in the clinic. This study highlights the importance of incorporating a molecular evaluation in the pediatric and adult epileptic neurosurgical population to further improve diagnosis and treatment and paves the way for clinical trials involving mTOR inhibitors.

Chapter 7: Conclusion

Overall, we successfully detected somatic mTOR pathway mutations in a higher proportion of patients than previously reported in the literature. Patients with an AAF at or below 1% continue to experience favourable seizure outcomes after their first surgery for a period of over two years post-resection. Additionally, for each patient, the mutation load correlated with histopathological classification, where clear or near clear resection borders resulted in favourable seizure outcomes. This study shows that resected tissue containing the most severe malformations on histopathology should be selected for somatic variant screening due to the increased probability of detecting pathogenic variants. Moreover, the detection of upregulated mutation present in the cDNA of FCD relative to DNA may suggest a positive feedback loop is at play in the pathology of FCD. Enhanced expression or retention of FCD variants in RNA relative to DNA may offer an easier way to obtain the diagnostic depth required to call variants and has the potential to offer enhanced detection in the clinic.

Our study demonstrates that developing and integrating a genetic-centred classification system for FCDs can provide a more comprehensive, reliable, and integrative genotype-phenotype diagnosis that could help further guide treatment options and enhance subsequent surgical interventions and pharmacologic therapies. Incorporating corresponding genetic and histopathological data into MRI computer-assisted presurgical assessment technology may also optimize surgical resection by improving MRI localization.

Integrating clinical screening for somatic mTOR pathway variants in FCD will have an immediate and direct impact on patient care and management. Identifying FCD patients who carry somatic mTOR pathway mutations is especially urgent given the clinical availability of mTOR pathway modulatory drugs.[8] Moreover, this study assists with the process of genetic

counselling as FCD patients with somatic mutations carry almost no risk of transmission to progeny.[31] Additionally, the identification of recurrent mutations in FCD may predict rapamycin sensitivity and aid in the development of hotspot testing to rapidly treat FCD patients in the clinic.[82]

Bibliography

1. Represa, A. (2019). Why malformations of cortical development cause epilepsy. *Frontiers in Neuroscience*, 13. https://doi.org/10.3389/fnins.2019.00250

2. Iffland, P., & Crino, P. (2017). Focal cortical dysplasia: Gene mutations, cell signaling, and therapeutic implications. *Annual Review of Pathology: Mechanisms of Disease*, *12*(1), 547-571. doi:10.1146/annurev-pathol-052016-100138

3. Prayson, R. (2018). *Pathology of Epilepsy. In Practical Surgical Neuropathology: A Diagnostic Approach (Second Edition)* (pp. 617–632). Philadelphia, PA: Elsevier. ISBN: 9780323449410

4. Kandel, E. R., Schwartz, J. H., & Jessell, T. M. (2000). *Principles of neural science* (4th ed.) (pp. 911-914). New York: McGraw-Hill, Health Professions Division. ISBN: 9780838577011

5. Wang, T., & Zhou, D. (2016). Non-invasive treatment options for focal cortical dysplasia. *Experimental and Therapeutic Medicine*, *11*(5), 1537-1541. doi: 10.3892/etm.2016.3100

6. Baldassari, S., Ribierre, T., Marsan, E., Adle-Biassette, H., Ferrand-Sorbets, S., Bulteau, C., Dorison, N., Fohlen, M., Polivka, M., Weckhuysen, S., Dorfmüller, G., Chipaux, M., & Baulac, S. (2019). Dissecting the genetic basis of focal cortical dysplasia: A large cohort study. *Acta Neuropathologica*, 138(6), 885–900. https://doi.org/10.1007/s00401-019-02061-5

7. Marsan, E., & Baulac, S. (2018). Review: Mechanistic target of rapamycin (mtor) pathway, focal cortical dysplasia and epilepsy. *Neuropathology and Applied Neurobiology*, 44(1), 6-17. doi:10.1111/nan.12463

8. Vilar, E., Perez-Garcia, J., & Tabernero, J. (2011). Pushing the envelope in the mTOR pathway: The second generation of inhibitors. *Molecular Cancer Therapeutics*, *10*(3), 395–403. https://doi.org/10.1158/1535-7163.MCT-10-0905

9. Patel, D., Tewari, B., Chaunsali, L., & Sontheimer, H. (2019). Neuron-glia interactions in the pathophysiology of epilepsy. *Nature Reviews Neuroscience*, *20*(5), 282-297. doi:10.1038/s41583-019-0126-4

10. Sirven, J. I. (2015). Epilepsy: A spectrum disorder. *Cold Spring Harbor Perspectives in Medicine*, *5*(9), a022848. https://doi.org/10.1101/cshperspect.a022848

11. Beghi, E. (2020). The epidemiology of epilepsy. *Neuroepidemiology*, 54(Suppl. 2), 185–191. https://doi.org/10.1159/000503831

12. Miller, J. W., & Goodkin, H. P. (Eds.). (2014). *Epilepsy: Miller/epilepsy*. John Wiley & Sons. https://doi.org/10.1002/9781118456989

13. Engel, J. (2014). Approaches to refractory epilepsy. *Annals of Indian Academy of Neurology*, *17*(5), 12. https://doi.org/10.4103/0972-2327.128644

14. Juric-Sekhar, G., & Hevner, R. F. (2019). Malformations of cerebral cortex development: Molecules and mechanisms. *Annual Review of Pathology*, *14*, 293–318. https://doi.org/10.1146/annurev-pathmechdis-012418-012927

15. Choi, S., & Kim, K. (2019). The surgical and cognitive outcomes of focal cortical dysplasia. *Journal of Korean Neurosurgical Society, 62*(3), 321-327. doi: 10.3340/jkns.2019.0005

16. Lee, W. S., Stephenson, S. E. M., Pope, K., Gillies, G., Maixner, W., Macdonald-Laurs, E., MacGregor, D., D'Arcy, C., Jackson, G., Harvey, A. S., Leventer, R. J., & Lockhart, P. J. (2020). Genetic characterization identifies bottom-of-sulcus dysplasia as an mTORopathy. *Neurology*, *95*(18), e2542–e2551. https://doi.org/10.1212/WNL.0000000000010670

17. Malley, C. O., & Pidgeon, G. P. (2016). The mTOR pathway in obesity driven gastrointestinal cancers: Potential targets and clinical trials. *BBA Clinical*, *5*, 29–40. https://doi.org/10.1016/j.bbacli.2015.11.003

18. Jesus-Ribeiro, J., Pires, L. M., Melo, J. D., Ribeiro, I. P., Rebelo, O., Sales, F., Freire, A., & Melo, J. B. (2021). Genomic and epigenetic advances in focal cortical dysplasia types i and ii: A scoping review. *Frontiers in Neuroscience*, *14*, 580357. https://doi.org/10.3389/fnins.2020.580357

19. Hidalgo, E. T., & Weiner, H. L. (2017). Surgery for epileptogenic cerebral dysplasia in children. *Developmental Medicine & Child Neurology*, *59*(3), 270–275. https://doi.org/10.1111/dmcn.13292

20. Oliveira-Manoel, A. L. (2020). Surgery for spontaneous intracerebral hemorrhage. *Critical Care*, 24(1), 45. https://doi.org/10.1186/s13054-020-2749-2

21. Taylor, D. C., Falconer, M. A., Bruton, C. J., & Corsellis, J. A. N. (1971). Focal dysplasia of the cerebral cortex in epilepsy. *Journal of Neurology, Neurosurgery & Psychiatry*, *34*(4),

369–387. https://doi.org/10.1136/jnnp.34.4.369

22. Kabat, J., & Król, P. (2012). Focal cortical dysplasia – review. *Polish Journal of Radiology*, *77*(2), 35–43.

23. Blümcke, I., Thom, M., Aronica, E., Armstrong, D. D., Vinters, H. V., Palmini, A., Jacques, T. S., Avanzini, G., Barkovich, A. J., Battaglia, G., Becker, A., Cepeda, C., Cendes, F., Colombo, N., Crino, P., Cross, J. H., Delalande, O., Dubeau, F., Duncan, J., … Spreafico, R. (2011). The clinicopathologic spectrum of focal cortical dysplasias: A consensus classification proposed by an ad hoc task force of the ilae diagnostic methods commission1: the ilae classification system of fcd. *Epilepsia*, *52*(1), 158–174. https://doi.org/10.1111/j.1528-1167.2010.02777.x

24. Blumcke, I., Spreafico, R., Haaker, G., Coras, R., Kobow, K., Bien, C., . . . Hartl, E. (2017). Histopathological findings in brain tissue obtained during epilepsy surgery. New England *Journal of Medicine*, 377(17). doi: 10.1056/NEJMoa1703784

25. Marin-Valencia, I., Guerrini, R., & Gleeson, J. (2014). Pathogenetic mechanisms of focal cortical dysplasia. *Epilepsia*, 55(7), 970-978. doi:10.1111/epi.12650

26. Najm, I. M., Sarnat, H. B., & Blümcke, I. (2018). Review: The international consensus classification of Focal Cortical Dysplasia - a critical update 2018. *Neuropathology and Applied Neurobiology*, *44*(1), 18–31. https://doi.org/10.1111/nan.12462

27. Bonduelle, T., Hartlieb, T., Baldassari, S., Sim, N. S., Kim, S. H., Kang, H.-C., Kobow, K., Coras, R., Chipaux, M., Dorfmüller, G., Adle-Biassette, H., Aronica, E., Lee, J. H., Blumcke, I., & Baulac, S. (2021). Frequent SLC35A2 brain mosaicism in mild malformation of cortical development with oligodendroglial hyperplasia in epilepsy (Moghe). *Acta Neuropathologica Communications*, *9*(1), 3. https://doi.org/10.1186/s40478-020-01085-3

28. Pritchard, D. J., & Korf, B. R. (2013). *Medical genetics at a glance* (3rd ed). John Wiley & Sons. ISBN: 9781118689011

29. Laddach, A., Ng, J. C. F., & Fraternali, F. (2021). Pathogenic missense protein variants affect different functional pathways and proteomic features than healthy population variants. *PLOS Biology*, *19*(4), e3001207. https://doi.org/10.1371/journal.pbio.3001207

30. Li, M. M., Datto, M., Duncavage, E. J., Kulkarni, S., Lindeman, N. I., Roy, S., Tsimberidou,

A. M., Vnencak-Jones, C. L., Wolff, D. J., Younes, A., & Nikiforova, M. N. (2017). Standards and guidelines for the interpretation and reporting of sequence variants in cancer. *The Journal of Molecular Diagnostics*, *19*(1), 4–23. https://doi.org/10.1016/j.jmoldx.2016.10.002

31. Moody, E. W., Vagher, J., Espinel, W., Goldgar, D., Hagerty, K. J., & Gammon, A. (2019). Comparison of somatic and germline variant interpretation in hereditary cancer genes. *JCO Precision Oncology*, *3*, 1–8. https://doi.org/10.1200/PO.19.00144

32. Verheijen, B. M., Vermulst, M., & van Leeuwen, F. W. (2018). Somatic mutations in neurons during aging and neurodegeneration. *Acta Neuropathologica*, *135*(6), 811–826. https://doi.org/10.1007/s00401-018-1850-y

33. D'Gama, A. M., Woodworth, M. B., Hossain, A. A., Bizzotto, S., Hatem, N. E., LaCoursiere, C. M., Najm, I., Ying, Z., Yang, E., Barkovich, A. J., Kwiatkowski, D. J., Vinters, H. V., Madsen, J. R., Mathern, G. W., Blümcke, I., Poduri, A., & Walsh, C. A. (2017). Somatic mutations activating the mtor pathway in dorsal telencephalic progenitors cause a continuum of cortical dysplasias. *Cell Reports*, *21*(13), 3754–3766. https://doi.org/10.1016/j.celrep.2017.11.106

34. Sallman, D. A., & Padron, E. (2016). Integrating mutation variant allele frequency into clinical practice in myeloid malignancies. *Hematology/Oncology and Stem Cell Therapy*, *9*(3), 89–95. https://doi.org/10.1016/j.hemonc.2016.04.003

35. Guerrini, R., Cavallin, M., Pippucci, T., Rosati, A., Bisulli, F., Dimartino, P., Barba, C., Garbelli, R., Buccoliero, A. M., Tassi, L., & Conti, V. (2021). Is focal cortical dysplasia/epilepsy caused by somatic *mtor* mutations always a unilateral disorder? *Neurology Genetics*, *7*(1), e540. https://doi.org/10.1212/NXG.0000000000000540

36. Lee, W. S., Baldassari, S., Chipaux, M., Adle-Biassette, H., Stephenson, S. E. M., Maixner, W., Harvey, A. S., Lockhart, P. J., Baulac, S., & Leventer, R. J. (2021). Gradient of brain mosaic RHEB variants causes a continuum of cortical dysplasia. *Annals of Clinical and Translational Neurology*, *8*(2), 485–490. https://doi.org/10.1002/acn3.51286

37. Lee, D. Y. (2015). Roles of mtor signaling in brain development. *Experimental Neurobiology*, *24*(3), 177–185. https://doi.org/10.5607/en.2015.24.3.177

38. Saxton, R. A., & Sabatini, D. M. (2017). Mtor signaling in growth, metabolism, and

disease. *Cell*, *168*(6), 960–976. https://doi.org/10.1016/j.cell.2017.02.004

39. Switon, K., Kotulska, K., Janusz-Kaminska, A., Zmorzynska, J., & Jaworski, J. (2017). Molecular neurobiology of mtor. *Neuroscience, 341*, 112-153. doi:10.1016/j.neuroscience.2016.11.017

40. Holz, M. K., Ballif, B. A., Gygi, S. P., & Blenis, J. (2005). Mtor and s6k1 mediate assembly of the translation preinitiation complex through dynamic protein interchange and ordered phosphorylation events. *Cell*, *123*(4), 569–580. https://doi.org/10.1016/j.cell.2005.10.024

41. Dennis, M. D., Jefferson, L. S., & Kimball, S. R. (2012). Role of p70s6k1-mediated phosphorylation of eif4b and pdcd4 proteins in the regulation of protein synthesis. *Journal of Biological Chemistry*, *287*(51), 42890–42899. https://doi.org/10.1074/jbc.M112.404822

42. Puighermanal, E., Biever, A., Pascoli, V., Melser, S., Pratlong, M., Cutando, L., Rialle, S., Severac, D., Boubaker-Vitre, J., Meyuhas, O., Marsicano, G., Lüscher, C., & Valjent, E. (2017). Ribosomal protein s6 phosphorylation is involved in novelty-induced locomotion, synaptic plasticity and mrna translation. *Frontiers in Molecular Neuroscience, 10*, 419. https://doi.org/10.3389/fnmol.2017.00419

43. Yoon, M.-S. (2017). The role of mammalian target of rapamycin (Mtor) in insulin signaling. *Nutrients*, *9*(11), 1176. https://doi.org/10.3390/nu9111176

44. Crino P. B. (2007). Focal brain malformations: a spectrum of disorders along the mTOR cascade. *Novartis Foundation symposium*, *288*, 260–281. doi:10.1002/9780470994030.ch18

45. Crino, P. (2015). Mtor signaling in epilepsy: Insights from malformations of cortical development. *Cold Spring Harbor Perspectives in Medicine, 5*(4). doi:10.1101/cshperspect.a022442

46. Fauser, S., Becker, A., Schulze-Bonhage, A., Hildebrandt, M., Tuxhorn, I., Pannek, H. W., Lahl, R., Schramm, J., & Blümcke, I. (2004). CD34-immunoreactive balloon cells in cortical malformations. *Acta Neuropathologica*, *108*(4), 272–278. https://doi.org/10.1007/s00401-004-0889-0

47. Lim, J. S., Kim, W., Kang, H.-C., Kim, S. H., Park, A. H., Park, E. K., Cho, Y.-W., Kim, S., Kim, H. M., Kim, J. A., Kim, J., Rhee, H., Kang, S.-G., Kim, H. D., Kim, D., Kim, D.-S., & Lee, J. H. (2015). Brain somatic mutations in MTOR cause focal cortical dysplasia

type II leading to intractable epilepsy. *Nature Medicine*, *21*(4), 395–400. https://doi.org/10.1038/nm.3824

48. Pelorosso, C., Watrin, F., Conti, V., Buhler, E., Gelot, A., Yang, X., Mei, D., McEvoy-Venneri, J., Manent, J.-B., Cetica, V., Ball, L. L., Buccoliero, A. M., Vinck, A., Barba, C., Gleeson, J. G., Guerrini, R., & Represa, A. (2019). Somatic double-hit in MTOR and RPS6 in hemimegalencephaly with intractable epilepsy. *Human Molecular Genetics*, *28*(22), 3755–3765. https://doi.org/10.1093/hmg/ddz194

49. Zhao, S., Li, Z., Zhang, M., Zhang, L., Zheng, H., Ning, J., Wang, Y., Wang, F., Zhang, X., Gan, H., Wang, Y., Zhang, X., Luo, H., Bu, G., Xu, H., Yao, Y., & Zhang, Y. (2019). A brain somatic RHEB doublet mutation causes focal cortical dysplasia type II. *Experimental & Molecular Medicine*, *51*(7), 1–11. https://doi.org/10.1038/s12276-019-0277-4

50. Rodin, R. E., & Walsh, C. A. (2018). Somatic mutation in pediatric neurological diseases. *Pediatric Neurology*, *87*, 20–22. https://doi.org/10.1016/j.pediatrneurol.2018.08.008

51. Chen, C.-J., Sgritta, M., Mays, J., Zhou, H., Lucero, R., Park, J., Wang, I.-C., Park, J. H., Kaipparettu, B. A., Stoica, L., Jafar-Nejad, P., Rigo, F., Chin, J., Noebels, J. L., & Costa-Mattioli, M. (2019). Therapeutic inhibition of mTORC2 rescues the behavioral and neurophysiological abnormalities associated with Pten-deficiency. *Nature Medicine*, *25*(11), 1684–1690. https://doi.org/10.1038/s41591-019-0608-y

52. Stiles, J., & Jernigan, T. L. (2010). The basics of brain development. *Neuropsychology Review*, *20*(4), 327–348. https://doi.org/10.1007/s11065-010-9148-4

53. Agirman, G., Broix, L., & Nguyen, L. (2017). Cerebral cortex development: An outside-in perspective. *FEBS Letters*, *591*(24), 3978–3992. https://doi.org/10.1002/1873-3468.12924

54. He, S., Li, Z., Ge, S., Yu, Y.-C., & Shi, S.-H. (2015). Inside-out radial migration facilitates lineage-dependent neocortical microcircuit assembly. *Neuron*, *86*(5), 1159–1166. https://doi.org/10.1016/j.neuron.2015.05.002

55. Subramanian, L., Calcagnotto, M., & Paredes, M. (2019). Cortical malformations: Lessons in human brain development. *Frontiers in Cellular Neuroscience*, *13*, 576-576. doi:10.3389/fncel.2019.00576

56. Barkovich, A. J., Guerrini, R., Kuzniecky, R. I., Jackson, G. D., & Dobyns, W. B. (2012). A developmental and genetic classification for malformations of cortical development: Update 2012. *Brain: A Journal of Neurology*, *135*(Pt 5), 1348–1369. https://doi.org/10.1093/brain/aws019

57. Fisher, R. S. (2017). The new classification of seizures by the international league against epilepsy 2017. *Current Neurology and Neuroscience Reports*, 17(6), 48. https://doi.org/10.1007/s11910-017-0758-6

58. Stafstrom, C. E., & Carmant, L. (2015). Seizures and epilepsy: An overview for neuroscientists. *Cold Spring Harbor Perspectives in Medicine*, *5*(6). https://doi.org/10.1101/cshperspect.a022426

59. Löscher, W., Potschka, H., Sisodiya, S. M., & Vezzani, A. (2020). Drug resistance in epilepsy: Clinical impact, potential mechanisms, and new innovative treatment options. *Pharmacological Reviews*, *72*(3), 606–638. https://doi.org/10.1124/pr.120.019539

60. Engel, J. (Ed.). (1993). *Surgical treatment of the epilepsies* (2nd ed). Raven Press.

61. Grabiner, B. C., Nardi, V., Birsoy, K., Possemato, R., Shen, K., Sinha, S., Jordan, A., Beck, A. H., & Sabatini, D. M. (2014). A diverse array of cancer-associated *mtor* mutations are hyperactivating and can predict rapamycin sensitivity. *Cancer Discovery*, *4*(5), 554–563. https://doi.org/10.1158/2159-8290.CD-13-0929

62. Park, S., Sim, H., & Lee, K. (2016). Rapamycin-resistant and torin-sensitive mtor signaling promotes the survival and proliferation of leukemic cells. *Bmb Reports*, *49*(1), 63-68. doi: 10.5483/BMBRep.2016.49.1.201

63. Christensen, C., Bonham, M. J., Wang, S., Ren, P., Martin, M., Jessen, K., Feldman, M. E., Weissman, J. S., Shokat, K. M., Rommel, C., & Ruggero, D. (2012). The translational landscape of mTOR signalling steers cancer initiation and metastasis. *Nature*, *485*(7396), 55–61. https://doi.org/10.1038/nature10912

64. Xu, Q., Uliel-Sibony, S., Dunham, C., Sarnat, H., Flores-Sarnat, L., Brunga, L., Davidson, S., Lo, W., Shlien, A., Connolly, M., Boelman, C., & Datta, A. (2019). Mtor inhibitors as a new therapeutic strategy in treatment resistant epilepsy in hemimegalencephaly: A case report. *Journal of Child Neurology*, *34*(3), 132–138. https://doi.org/10.1177/0883073818813238

65. Palavra, F., Robalo, C., & Reis, F. (2017). Recent advances and challenges of mtor inhibitors use in the treatment of patients with tuberous sclerosis complex. *Oxidative Medicine and Cellular Longevity, 2017*, 9820181-9820181. doi:10.1155/2017/9820181

66. Ohne, Y., Takahara, T., Hatakeyama, R., Matsuzaki, T., Noda, M., Mizushima, N., & Maeda, T. (2008). Isolation of hyperactive mutants of mammalian target of rapamycin. *The Journal of Biological Chemistry, 283*(46), 31861-70. doi:10.1074/jbc.M801546200

67. Williams, M., DeSpenza, T., Li, M., Gulledge, A., & Luikart, B. (2015). Hyperactivity of newborn pten knock-out neurons results from increased excitatory synaptic drive. *The Journal of Neuroscience: The Official Journal of the Society for Neuroscience, 35*(3), 943-59. doi:10.1523/JNEUROSCI.3144-14.2015

68. Ak, H., Ay, B., Tanriverdi, T., Sanus, G. Z., Is, M., Sar, M., … Uzan, M. (2007). Expression and cellular distribution of multidrug resistance-related proteins in patients with focal cortical dysplasia. *Seizure, 16*(6), 493–503. doi: 10.1016/j.seizure.2007.03.011

69. Abdijadid, S., Mathern, G., Levine, M., & Cepeda, C. (2015). Basic mechanisms of epileptogenesis in pediatric cortical dysplasia. *Cns Neuroscience & Therapeutics, 21*(2), 92-103. doi:10.1111/cns.12345

70. Calcagnotto, M., Paredes, M., Tihan, T., Barbaro, N., & Baraban, S. (2005). Dysfunction of synaptic inhibition in epilepsy associated with focal cortical dysplasia. *The Journal of Neuroscience : The Official Journal of the Society for Neuroscience, 25*(42), 9649-57. doi: 10.1523/JNEUROSCI.2687-05.2005

71. Park, S. M., Lim, J. S., Ramakrishina, S., Kim, S. H., Kim, W. K., Lee, J., Kang, H.-C., Reiter, J. F., Kim, D. S., Kim, H. (Henry), & Lee, J. H. (2018). Brain somatic mutations in mtor disrupt neuronal ciliogenesis, leading to focal cortical dyslamination. *Neuron*, *99*(1), 83-97.e7. https://doi.org/10.1016/j.neuron.2018.05.039

72. Nguyen, L. H., Mahadeo, T., & Bordey, A. (2019). Mtor hyperactivity levels influence the severity of epilepsy and associated neuropathology in an experimental model of tuberous sclerosis complex and focal cortical dysplasia. *The Journal of Neuroscience: The Official Journal of the Society for Neuroscience*, *39*(14), 2762–2773. https://doi.org/10.1523/JNEUROSCI.2260-18.2019

73. Li, L., Liu, C.-Q., Li, T.-F., Guan, Y.-G., Zhou, J., Qi, X.-L., Yang, Y.-T., Deng, J.-H., Xu,

Z.-Q. D., & Luan, G.-M. (2016). Analysis of altered micro rna expression profiles in focal cortical dysplasia iib. *Journal of Child Neurology*, *31*(5), 613–620. https://doi.org/10.1177/0883073815609148

74. Chen, S.-D., Pan, H.-Y., Huang, J.-B., Liu, X.-P., Li, J.-H., Ho, C.-J., Tsai, M.-H., Yang, J.-L., Chen, S.-F., Chen, N.-C., & Chuang, Y.-C. (2020). Circulating micrornas from serum exosomes may serve as a putative biomarker in the diagnosis and treatment of patients with focal cortical dysplasia. *Cells*, *9*(8). https://doi.org/10.3390/cells9081867

75. Ravizza, T., & Vezzani, A. (2018). Pharmacological targeting of brain inflammation in epilepsy: Therapeutic perspectives from experimental and clinical studies. *Epilepsia Open, 3*, 133-142. doi:10.1002/epi4.12242

76. Maroso, M., Balosso, S., Ravizza, T., Iori, V., Wright, C., French, J., & Vezzani, A. (2011). Interleukin-1β biosynthesis inhibition reduces acute seizures and drug resistant chronic epileptic activity in mice. *Neurotherapeutics : The Journal of the American Society for Experimental Neurotherapeutics, 8*(2), 304-15. doi:10.1007/s13311-011-0039-z

77. Møller, R., Weckhuysen, S., Chipaux, M., Marsan, E., Taly, V., Bebin, E., . . . Baulac, S. (2016). Germline and somatic mutations in the mtor gene in focal cortical dysplasia and epilepsy. *Neurology. Genetics, 2*(6), 118. doi: 10.1212/NXG.0000000000000118

78. Rohlin, A., Wernersson, J., Engwall, Y., Wiklund, L., Björk, J., & Nordling, M. (2009). Parallel sequencing used in detection of mosaic mutations: Comparison with four diagnostic dna screening techniques. *Human Mutation, 30*(6), 1012-1020. doi:10.1002/humu.20980

79. Thomas, P., & Smart, T. (2005). Hek293 cell line: A vehicle for the expression of recombinant proteins. *Journal of Pharmacological and Toxicological Methods, 51*(3), 187-200. doi:10.1016/j.vascn.2004.08.014

80. Kobow, K., Ziemann, M., Kaipananickal, H., Khurana, I., Mühlebner A, Feucht, M., … Kaspi, A. (2019). Genomic dna methylation distinguishes subtypes of human focal cortical dysplasia. *Epilepsia*, *60*(6), 1091–1103. https://doi.org/10.1111/epi.14934

81. Vogl, C., Mochida, S., Wolff, C., Whalley, B. J., & Stephens, G. J. (2012). The synaptic vesicle glycoprotein 2a ligand levetiracetam inhibits presynaptic ca2 channels through an intracellular pathway. *Molecular Pharmacology*, *82*(2), 199–208. https://doi.org/10.1124/mol.111.076687

82. Chen, T., Wang, Z., Zhou, W., Chong, Z., Meric-Bernstam, F., Mills, G. B., & Chen, K. (2016). Hotspot mutations delineating diverse mutational signatures and biological utilities across cancer types. *Bmc Genomics*, *17*, 394–394. https://doi.org/10.1186/s12864-016-2727-x

83. Rogozin, I. B., & Pavlov, Y. I. (2003). Theoretical analysis of mutation hotspots and their dna sequence context specificity. *Mutation Research*, *544*(1), 65–85. doi: 10.1016/s1383-5742(03)00032-2

84. Hardt, M., Chantaravisoot, N., & Tamanoi, F. (2011). Activating mutations of tor (target of rapamycin). *Genes to Cells : Devoted to Molecular & Cellular Mechanisms, 16*(2), 141-51. doi:10.1111/j.1365-2443.2010.01482.x

85. Yang, H., Rudge, D. G., Koos, J. D., Vaidialingam, B., Yang, H. J., & Pavletich, N. P. (2013). Mtor kinase structure, mechanism and regulation. *Nature*, *497*(7448), 217–223. https://doi.org/10.1038/nature12122

86. Miled, N., Yan, Y., Hon, W., Perisic, O., Zvelebil, M., Inbar, Y., . . . Williams, R. (2007). Mechanism of two classes of cancer mutations in the phosphoinositide 3-kinase catalytic subunit. *Science, 317*(5835), 239-242. doi: 10.1126/science.1135394

87. Zhang, Z., Gao, K., Liu, Q., Zhou, J., Li, X., Lang, N., … Wu, Y. (2020). Somatic variants in new candidate genes identified in focal cortical dysplasia type ii. *Epilepsia*, *61*(4), 667–678. https://doi.org/10.1111/epi.16481

88. Zou, Z., Tao, T., Li, H., & Zhu, X. (2020). Mtor signaling pathway and mtor inhibitors in cancer: Progress and challenges. *Cell & Bioscience*, *10*, 31. https://doi.org/10.1186/s13578-020-00396-1

89. Mira, H., & Morante, J. (2020). Neurogenesis from embryo to adult—Lessons from flies and mice. *Frontiers in Cell and Developmental Biology*, *8*, 533. https://doi.org/10.3389/fcell.2020.00533

90. Lizhong, D., Ethan, R., & Yongsheng, B. (2017). Comparison of alternative splicing junction detection tools using rnaseq data. *Current Genomics, 18*(3), 268-277. doi:10.2174/1389202918666170215125048

91. Ganji, Z., Hakak, M. A., Zamanpour, S. A., & Zare, H. (2021). Automatic detection of focal

cortical dysplasia type ii in mri: Is the application of surface-based morphometry and machine learning promising? *Frontiers in Human Neuroscience*, *15*, 608285. https://doi.org/10.3389/fnhum.2021.608285

Appendices

Plasmid	Tag	Vector Backbone
Flag-mTOR WT	FLAG (N terminal on insert)	pcDNA3
HA-S6K1	HA/GST (N terminal on backbone)	pRK5
Empty vector	Myc (N terminal on backbone)	pRK7
Patient 10) c.4373_4375dupATG, p.Asp1458dup	FLAG (N terminal on insert)	pcDNA3
Patient 9) c.7499T>A, p.Ile2500Asn	FLAG (N terminal on insert)	pcDNA3
pcDNA3-FLAG-MTOR-Leu1460Pro (Known mTOR pathway upregulation variant from Addgene repository)	FLAG (N terminal on backbone)	pcDNA3
pcDNA3-FLAG-MTOR-Ile2500Phe (Known mTOR pathway upregulation variant from Addgene repository)	FLAG (N terminal on backbone)	pcDNA3

Table S1: List of plasmids and their corresponding tags.

In total, seven plasmids were used in transient co-transfection functional studies. Plasmids flag-mTOR-Leu1460Pro, and flag-mTOR-Ile2500Phe, were selected from the Addgene repository due to the proximity of their mutated site to the variants identified in Patients 9 and 10.

FCD subtype	Gene	Nucleotide and protein change	Inheritance
FCD I	*DEPDC5*	c.715C>T (p.Arg239*) + c.1264C>T (p.Arg422*)	Germline (inherited) + Somatic
	PCDH19	duplication of exons 3,4,5a	Germline (de novo)
FCD Ia	*STXBP1*	c.1631G>T (p.Gly544Val)	Germline (de novo)
	SCN1A	c.317C>T (p.Ser106Phe)	Germline (inherited)
	NPRL2	c.68_69delCT (p.Ile23Asnfs*6)	Germline
	KCNT1	c.2800G>A (p.Ala934Thr)	Germline (de novo)
	SLC35A2	c.339_340insCTC (p.Leu113dup) c.634_635del (p.Ser212Leufs*9)	All somatic
FCD Ib	*AKT3*	duplication of chromosome. 1q21.1-q44	Somatic
	STXBP1	exons 3–4 deletion	Germline (de novo) +Somatic
	KCNT1	c.2849G>A (p.Arg950Gln) c.2386T>C (p.Tyr796His)	Germline (inherited)
FCD Ic	*DEPDC5*	c.1310delA (p.Asn437Metfs*21)	Germline (inherited)

Table S2: Summary of all variants previously reported in FCD type I. (Adapted from[18])

FCD subtype	Gene	Nucleotide and protein change	Inheritance	Publication Reference (author, journal, year)
FCD IIa	*MTOR*	c.7280T>C (p.Leu2427Pro); c.6577C>T (p.Arg2193Cys); c.1871G>A (p.Arg624His); c.5126G>A (p.Arg1709His)	All somatic	Lim et al., Nat Med., 2015
		c.4487T>G (p.Trp1456Gly)	Somatic	Leventer et al., Neurology, 2015
		c.4379T>C (p.Leu1460Pro) c.6644C>T (p.Ser2215Phe) c.6644C>A (p.Ser2215Tyr)	All somatic	Mirzaa et al., JAMA Neurol., 2016
		c.6644C>T (p.Ser2215Phe) c.6644C>A (p.Ser2215Tyr)	All somatic	Moller et al., Neurol Genet., 2016
		c.4376C>A (p.Ala1459Asp) c.4379 T>C (p.Leu1460Pro) c.6644C>T (p.Ser2215Phe) c.6644C>A (p.Ser2215Tyr) c.7498A>T (p.Ile2500Phe)	All somatic	Baldassari et al., Acta Neuropathol., 2019
		c.1871G>A (p.Arg624His) c.5126G>A (p.Arg1709His) c.5930C>A (p.Thr1977Lys) c.7280T>C (p.Leu2427Pro) c.6577C>T (p.Arg2193Cys) c.6644C>T (p.Ser2215Phe) c.4379T>C (p.Leu1460Pro) c.6400C>T (p.Arg2134Trp)	All somatic	Sim et al., Acta Neuropathol., 2019
	PIK3CA	c.3139C>T (p.His1047Arg)	Somatic	Jansen et al., Brain, 2015
	AKT1	c.1099C>T (p.Arg367Cys)	n.a.	Kobow et al., Epilepsia, 2019
	AKT3	c.49G>A (p.Glu17Lys)	Somatic	Baldassari et al., Acta Neuropathol., 2019
	TSC1	c.610C>T (p.Arg204Cys) c.64C>T (p.Arg22Trp)	All somatic	Lim et al., Am J Hum Genet., 2017
		c.610C>T (p.Arg204Cys) c.64C>T (p.Arg22Trp)	All somatic	Sim et al., Acta Neuropathol., 2019
	TSC 2	c.4639G>A (p.Val1547Ile)	Somatic	Lim et al., Am J Hum Genet., 2017
		c.4639G>A (p.Val1547Ile)	Somatic	Sim et al., Acta Neuropathol., 2019
	RHEB	c.104A>T,105C>A (p.Tyr35Leu)	Doublet somatic	Zhao et al., Exp Mol Med., 2019
	DEPDC5	c.484-1G>A (p.?) c.1759C>T (p.Arg587*)	Germline mosaic Germline (inherited)	Baulac et al., Ann Neurol., 2015
		c.1663C>T (p.Arg555*)	Germline (inherited)	Scerri et al., Ann Clin Transl Neurol.,2015
		c.842A>T (p.Tyr281Phe)	Germline (inherited)	Carvill et al., Neurol Genet., 2015
		c.2620C>T (p.Arg874*)	Germline	D'Gama et al.,Cell Rep., 2017
		c.856C>T (p.Arg286*) + c.865C>T (p.Gln289*)	Germline (inherited) + 2-hit somatic	Ribierre et al., J Clin Investig., 2018
		c.2390delA (p.Gln797Argfs*18) + c.3994C > T (p.Arg1332*)	Germline (de novo) + 2-hit somatic	Lee et al., Ann Clin Transl Neurol., 2019
		c.279+1G>A (p.?) c.1264C>T (p.Arg422*)	Germline (inherited) Germline (inherited)	Baldassari et al., Genet Med., 2019
		c.856C >T (p.Arg286*) + c.865C>T (p.Gln289*) c.279 + 1G >A (p.?) c.715C>T (p.Arg239*) c.3021 + 1G >A (p.?) + c.4151_4152insC (p.Glu1385fs)	Germline + 2-hit somatic Germline Germline Germline + somatic Germline	Baldassari et al., Acta Neuropathol., 2019
		c.1114C>T (p.Gln372*) c.3639G>A (p.Trp1213*) c.3802C>T (p.Arg1268*) c.3406A>T (p.Arg1136*)	All germline	Sim et al., Acta Neuropathol., 2019
		c.483 + 1G>A	Germline	Kobow et al., Epilepsia, 2019
		c.3225_3226insGAAAGGT (p.Asp1075fs)	Germline	Ying et al., Epileptic Disord., 2019
	NPRL2	c.562C>T (p.Gln188*)	Germline	D'Gama et al.,Cell Rep., 2017
		c.100C>T (p.Arg34*) c.683+1G>C (p.?)	Germline (inherited) Germline	Baldassari et al., Genet Med., 2019
	NPRL3	c.1375_1376dupAC (p.Ser460Profs*20) c.1352-4delACAGinsTGACCCATCC c.275G>A (p.Arg92Gln)	All germline	Sim et al., Ann Neurol., 2016
		c.1270C>T (p.Arg424*)	Germline	Weckhuysen et al., Epilepsia, 2016
	DEPTOR	c.338T>A (p.Leu113His)	Germline (inherited)	Scerri et al., Ann Clin Transl Neurol.,2015
	SCN1A	c.2584C>G (p.Arg862Gly)	Germline (de novo)	Barba et al., Epilepsia, 2014
	PCDH19	c.696T>A (p.Asn232Lys)	Germline (de novo)	Kurian et al., Dev Med Child Neurol., 2018

	RAB6B	**c.383C>T (p.Thr128Met)**	**Somatic**	**Zhang et al., Epilepsia, 2020**
FCD IIb	***MTOR***	**c.6644C>T (p.Ser2215Phe); c.7280T>A (p.Leu2427Gln); c.5930C>A (p.Thr1977Lys); c.4348T>G (p.Tyr1450Asp); c.4447T>C (p.Cys1483Arg)**	**All somatic**	**Lim et al., Nat Med., 2015**
		c.6644C>A (p.Ser2215Tyr) c.4376C>A (p.Ala1459Asp) c.4379T>C (p.Leu1460Pro) c.6644C>T (p.Ser2215Phe)	**All somatic**	**Nakashima et al., Ann Neurol., 2015**
		c.6644C>T (p.Ser2215Phe) c.6644C>A (p.Ser2215Tyr) c.4379T>C (p.Leu1460Pro) c.4375G>T (p.Ala1459Ser)	**All somatic**	**Moller et al., Neurol Genet., 2016**
		c.4379T>C (p.Leu1460Pro) c.4447T>C (p.Cys1483Arg)	**All somatic**	**D'Gama et al., Cell Rep., 2017**
		c.4379T>C (p.Leu1460Pro)	**Somatic**	**Avansini et al., Ann Neurol., 2018**
		c.4376C>A (p.Ala1459Asp) c.4379 T>C (p.Leu1460Pro) c.5930C>A (p.Thr1977Lys) c.6644C>T (p.Ser2215Phe) c.6644C>A (p.Ser2215Tyr)	**All somatic**	**Baldassari et al., Acta Neuropathol., 2019**
		c.6644C>T (p.Ser2215Phe) c.7280T>A (p.Leu2427Gln) c.5930C>A (p.Thr1977Lys) c.4348T>G (p.Tyr1450Asp) c.4447T>C (p.Cys1483Arg) c.4366T>G(p.Trp1456Gly) c.4376C>A (p.Ala1459Asp) c.6644C>A (p.Ser2215Tyr)	**All somatic**	**Sim et al., Acta Neuropathol., 2019**
		c.5930C>A (p.Thr1977Lys);	**Somatic**	**Zhang et al., Epilepsia, 2020**
	PIK3C3	**c.760A>G (p.Lys254Glu)**	**Germline**	**D'Gama et al., Ann Neurol., 2015**
	PIK3C2B	**c.3011C>G (p.Ala1004Gly)**	**Germline**	**D'Gama et al., Ann Neurol., 2015**
	PTEN	**c.834C>G (p.Phe278Leu)**	**Somatic**	**Schick et al., Acta Neuropathol., 2006**
	AKT1	**C.349_351del(p.Glu117del)**	**Somatic**	**Avansini et al., Ann Neurol., 2018**
	TSC1	**c.453G>A (p.Glu78Lys) c.549 G>A (p.Ala110Thr) c.2415C>T (p.His732Tyr)**	**-**	**Becker et al., Ann Neurol., 2002**
		c.64C>T (p.Arg22Trp)	**Somatic**	**Lim et al., Am J Hum Genet., 2017**
		c.163C>T (p.Gln55*)	**Somatic**	**D'Gama et al.,Cell Rep., 2017**
		c.1525C >T (p.Arg509*) c.1907_1908delAG (p.Glu636fs*51)	**All somatic**	**Baldassari et al., Acta Neuropathol., 2019**
		c.64C>T (p.Arg22Trp) c.2074C>T (p.Arg692*) c.1525C>T (p.Arg509*)	**All somatic**	**Sim et al., Acta Neuropathol., 2019**
	TSC2	**c.3781G>A (p.Ala1261Thr)**	**Somatic**	**Avansini et al., Ann Neurol., 2018**
		c.5228G >A (p.Arg1743Gln) c.2380C>T (p.Gln794*)	**All somatic**	**Baldassari et al., Acta Neuropathol., 2019**
		c.1372C>T (p.Arg458*)	**Somatic**	**Sim et al., Acta Neuropathol., 2019**
		c.5227C>T (p.Arg1743Trp)	**Somatic**	**Zhang et al., Epilepsia, 2020**
	RHEB	**c.119A >T (p.Glu40Val)**	**Somatic**	**Baldassari et al., Acta Neuropathol., 2019**
	DEPDC5	**c.783_786delTGAG (p.Asn261Lysfs*11) c.624+1G>A (p.?) c.1218-18_1218-15delTGTT (p.?) c.1355C>T (p.Ala452Val)**	**All germline**	**D'Gama et al., Ann Neurol., 2015**
		c.1400_1401insGG (pPhe467Leufs*51)	**Germline (inherited)**	**Baldassari et al., Genet Med., 2019**
		c.4521_4522delAA (p.Thr1508fs) + c.4162_4169dupGTACTCTT (p.Phe1399fs)	**Germline + 2-hit somatic**	**Sim et al., Acta Neuropathol., 2019**
	IRS1	**c.1791dupG (p.His598Ala fs*13)**	**Somatic**	**Zhang et al., Epilepsia, 2020**
	ZNF337	**c.692_693del (p.Thr231Arg fs*45)**	**Somatic**	**Zhang et al., Epilepsia, 2020**
	HTR6	**c.469G>A (p.Ala157Thr)**	**Somatic**	**Zhang et al., Epilepsia, 2020**
	RALA	**c.482G>A (p.Arg161Gln)**	**Somatic**	**Zhang et al., Epilepsia, 2020**

Table S3: Summary of all variants previously reported in FCD type II. (Adapted from[18])